Synthesis of d^2 Complexes That Contain $[W(NAr)_2]$ and $[Re(NAr)_2]$ Cores, SCF-Xα-SW Calculations, and a Discussion of the $MCp_2/M'(NR)_2$ Isolobal Relationship

Darryl S. Williams, Mark H. Schofield, and Richard R. Schrock*

Department of Chemistry 6-331, Massachusetts Institute of Technology, Cambridge, Massachusetts 02139

Received June 2, 1993®

$W(NAr)_2Cl_2(dme)$ is reduced by sodium amalgam in the presence of a phosphine in THF to give $W(NAr)_2(PMe_2Ph)_2$ (**1a**) or $W(NAr)_2(PMePh_2)_2$ (**1b**). An X-ray study of **1b** showed that the geometry about tungsten is nearly tetrahedral with P—W—N bond angles of 107° (average), a N—W—N angle of 128.8(2)°, and a P—W—P angle of 94.60 (6)°; the W=N bond lengths are identical and consistent with their being pseudotriple bonds, and the W=N—Ar bond angles are almost linear (166 and 172°). $W(NAr)_2(PMe_2Ph)_2$ reacts readily with ethylene to form orange $W(NAr)_2(PMe_2Ph)_2(\eta^2\text{-}C_2H_4)$, with acetylene to form dark red $W(NAr)_2(PMe_2Ph)_2(\eta^2\text{-}C_2H_2)$, and with (trimethylsilyl)acetylene to form $W(NAr)_2(PMe_2Ph)(\eta^2\text{-}HC{\equiv}CSiMe_3)$. Addition of norbornene to **1a** gives $W(NAr)_2(PMe_2Ph)(\eta^2\text{-norbornene})$, while addition of acetone, propionaldehyde, or cyclopentanone gives orange-yellow $W(NAr)_2(PMe_2Ph)(\eta^2\text{-}OCMe_2)$ (**6a**), $W(NAr)_2(PMe_2Ph)(\eta^2\text{-}OCHEt)$, or $W(NAr)_2(PMe_2Ph)(\eta^2\text{-cyclopentanone})$. An X-ray study showed **6a** to have the proposed pseudotetrahedral structure in which W, P, O, and C all lie in the plane that bisects the N—W—N angle (mean deviation of 0.034 Å) and in which the C—O distance is 1.39(1) Å. Reduction of $Re(NAr)_2Cl_3(py)$ (Ar = 2,6-C_6H_3-*i*-Pr_2) with zinc or sodium amalgam in the presence of excess pyridine in tetrahydrofuran yields brown, microcrystalline $Re(NAr)_2(py)_2Cl$ (**7**). Compound **7** reacts with 2-butyne to yield $Re(NAr)_2(\eta^2\text{-MeC}{\equiv}\text{CMe})Cl$ and with phosphines to yield $Re(NAr)_2(L)(py)Cl$ (L = $PMePh_2$ (**9a**) or PPh_3 (**9b**)). Addition of thallium tetrafluoroborate to **9a** in the presence of $PMePh_2$ yields $[Re(NAr)_2(PMePh_2)_2][BF_4]$. Reduction of **7** in the presence of $PMePh_2$ gave $Re(NAr)_2(PMePh_2)_2H$ in low yield. Reduction of $Re(NAr)_2(CH_2\text{-}t\text{-Bu})Cl_2$ in THF in the presence of pyridine yields green $Re(NAr)_2(CH_2\text{-}t\text{-Bu})(py)_2$ (**12**). Compound **12** reacts rapidly with 2-butyne to give $Re(NAr)_2(CH_2\text{-}t\text{-Bu})(\eta^2\text{-MeC}{\equiv}\text{CMe})$ and with acetone, pivaldehyde, or norbornene to give $Re(NAr)_2(CH_2\text{-}t\text{-Bu})(\eta^2\text{-}OCMe_2)$, $Re(NAr)_2(CH_2\text{-}t\text{-Bu})(\eta^2\text{-}OCH\text{-}t\text{-Bu})$, or $Re(NAr)_2(CH_2\text{-}t\text{-Bu})(\eta^2\text{-norbornene})$, respectively. Reduction of $Re(NAr)_2(CH_2\text{-}t\text{-Bu})Cl_2$ in the presence of PMe_2Ph gave highly crystalline, diamagnetic $Re(NAr)_2(CH_2\text{-}t\text{-Bu})(PMe_2Ph)$ (**14**) in 80% yield. Compound **14** reacts with ethylene, acetylene, and carbon monoxide to give $Re(NAr)_2(CH_2\text{-}t\text{-Bu})(PMe_2Ph)(\eta^2\text{-}C_2H_4)$ (**15a**), $Re(NAr)_2(CH_2\text{-}t\text{-Bu})(PMe_2Ph)(\eta^2\text{-}C_2H_2)$ (**15b**), and $Re(NAr)_2(CH_2\text{-}t\text{-Bu})(CO)(PMe_2Ph)$ (**15c**), respectively. Compound **15b** rearranges readily to the "alkylidene" complex, $Re(NAr)_2(CH_2\text{-}t\text{-Bu})(CHCHPMe_2Ph)$. An analysis of the bonding in hypothetical $W(NH)_2(PH_3)_2$ by the SCF-Xα-SW method shows that the HOMO is a metal-centered nonbonding orbital ($7a_1$). As the N—M—N angle increases, the four nondegenerate π levels evolve into two sets of doubly-degenerate π orbitals, in agreement with calculated changes for MCp_2 complexes. Calculations on hypothetical $[Re(NH)_2(PH_3)_2]^+$ yielded similar results. The frontier orbitals of $M(NR)_2$ complexes and their isolobal relationship with $M'Cp_2$ complexes, supported by SCF-Xα-SW calculations, are discussed.

Introduction

Several years ago we reported in a preliminary fashion the synthesis of pseudotetrahedral and trigonal bipyramidal d^2 bis(arylimido) complexes of tungsten.[1] Pseudotetrahedral complexes that contain an η^2-ligand were found to have structures analogous to those observed for d^2 pseudotetrahedral metallocene complexes; i.e., the η^2-ligand lies in a plane that bisects the N—W—N angle. We proposed that even though the two imido ligands were not both strictly linear in the one crystallographically characterized complex, the imido ligands behaved as $2\pi,1\sigma$ ligands, i.e., the 14 electron $W(NR)_2$ core is analogous to a 14 electron $M(\eta^5\text{-}C_5R_5)_2$ core where M is a group 4 metal. Pseudotetrahedral d^2 complexes of the type $Re(NR)_2(\eta^2\text{-ligand})X$ (X is an anionic ligand) were found to have analogous "metallocene-like" structures.[2] In principle a variety of metallocene-like d^0 or d^2 complexes that contain two $2\pi,1\sigma$ ligands should be preparable; possibilities include $M(\eta^5\text{-}C_5R_5)(NR)$ complexes (M = group 5 metal), $M(\eta^5\text{-}C_5R_5)(CR')$ complexes (M = group 6 metal), and $M(CR)(NR')$ complexes (M = group 7 metal). In fact, a series of niobium and tantalum cyclopentadienyl/imido complexes have been prepared and shown to have metallocene-like structures.[3-8] Structurally characterized examples include $Nb(\eta^5\text{-}C_5Me_5)(NAr)(CHPh)(PMe_3)$ (Ar

* Abstract published in *Advance ACS Abstracts*, October 1, 1993.

(1) Williams, D. S.; Schofield, M. H.; Anhaus, J. T.; Schrock, R. R. *J. Am. Chem. Soc.* **1990**, *112*, 6728.

(2) Weinstock, I. A.; Schrock, R. R.; Williams, D. S.; Crowe, W. E. *Organometallics* **1991**, *10*, 1.

(3) Williams, D. N.; Mitchell, J. P.; Poole, A. D.; Siemeling, U.; Clegg, W.; Hockless, D. C. R.; O'Neil, P. A.; Gibson, V. C. *J. Chem. Soc., Dalton Trans.* **1992**, 739.

0276-7333/93/2312-4560$04.00/0

= 2,6-C_6H_3-*i*-Pr_2),[7] Nb(η^5-C_5H_5)(NAr)(benzyne)(PMe_3),[7] and Nb(η^5-C_5H_5)(NAr)(CH_2=CHMe)(PMe_3).[8] Photoelectron studies of Os(η^6-C_6H_6)(N-*t*-Bu) and Ir(η^5-C_5Me_5)(N-*t*-Bu) also have been reported that support the analogy between an imido ligand and a η^5-cyclopentadienyl ligand.[9]

In this paper we report the full details of the synthesis of some d^2 tungsten and rhenium bis(arylimido) complexes, along with SCF–Xα–SW calculations that support the metallocene analogy. We chose arylimido ligands since we have developed routes to d^0 bis(arylimido) complexes of Mo,[10,11] W,[12] and Re[13–15] and employed them as starting materials for the synthesis of alkylidene complexes. At this stage it is not clear how and to what extent the structure and chemistry of metallocene-like d^2 bis(arylimido) complexes might differ from bis(*tert*-butylimido) complexes.

Results

Synthesis of d^2 $W(NAr)_2$ Complexes (Ar = Diisopropylphenyl). $W(NAr)_2Cl_2(dme)$[12] is readily reduced by sodium amalgam in the presence of dimethylphenylphosphine in THF to give burgundy-colored, air-sensitive $W(NAr)_2(PMe_2Ph)_2$ (**1a**) in 50–60% yield. NMR

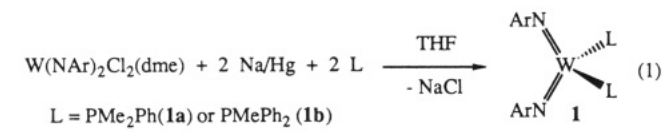

data are consistent with a highly symmetric structure in which the imido ligands are equivalent and the phosphine ligands are equivalent. ^{31}P NMR data indicate that the phosphine ligands are not lost readily from the metal on the NMR time scale in solution. However, added phosphine exchanges readily with coordinated phosphine on the NMR time scale, presumably via formation of $W(NAr)_2(PMe_2Ph)_3$. (See later for other five-coordinate species.) An analogous $PMePh_2$ complex, $W(NAr)_2(PMePh_2)_2$ (**1b**), was found to form crystals suitable for X-ray diffraction studies.

The molecular structure of **1b** is shown in Figure 1, and relevant bond lengths and angles are listed in Table I. Although there is no crystallographically imposed symmetry about the tungsten atom in **1b**, the W=N bond lengths are identical within experimental error and consistent with their being pseudotriple bonds, and the W=N—Ar bond angles are almost linear (166 and 172°). The geometry about tungsten is nearly tetrahedral with

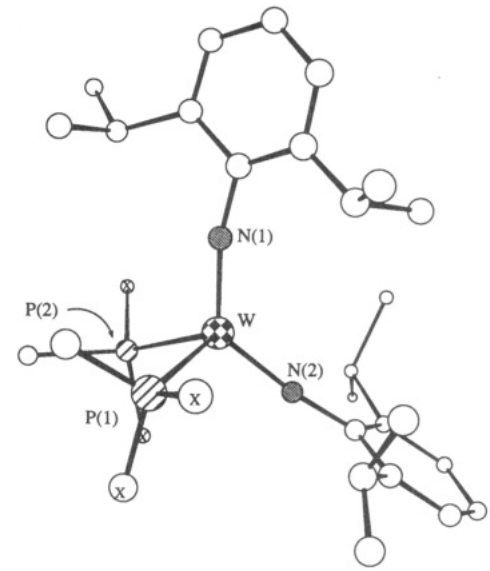

Figure 1. Molecular structure of $W(NAr)_2(PMePh_2)_2$ (**1b**). (Phosphine phenyl rings are omitted for clarity and ipso carbon atoms are marked with an X.)

Table I. Selected Bond Distances (Å) and Angles (deg) in $W(NAr)_2(PMePh_2)_2$ (1b)

	Distances		
W–N(1)	1.805(5)	W–P(1)	2.411(2)
W–N(2)	1.793(5)	W–P(2)	2.409(2)
	Angles		
P(1)–W–P(2)	94.60(6)	P(2)–W–N(2)	106.6(2)
P(1)–W–N(1)	108.58(2)	N(1)–W–N(2)	128.8(2)
P(1)–W–N(2)	106.5(2)	W–N(1)–C(11)	166.0(5)
P(2)–W–N(1)	106.6(2)	W–N(2)–C(21)	172.8(5)

P—W—N bond angles of 107° (average), a N—W—N angle of 128.8(2)°, and a P—W—P angle of 94.60(6)°. All such interligand angles are similar to those found in structurally-characterized d^2 group 4 metallocene complexes such as $Cp_2Ti(PMe_3)_2$.[16] The phenyl rings of the imido ligands lie in planes that are approximately perpendicular to one another, a circumstance that probably is favored for steric reasons.

$W(NAr)_2(PMe_2Ph)_2$ reacts readily with acetylenes or olefins to give products of a type that appears to depend largely on the size of the added ligand. For example, $W(NAr)_2(PMe_2Ph)_2$ reacts with ethylene to form orange needles of $W(NAr)_2(PMe_2Ph)_2(\eta^2$-$C_2H_4)$ (**2**) and with acetylene to form dark red needles of $W(NAr)_2(PMe_2Ph)_2(\eta^2$-$C_2H_2)$ (**3**). The two ends of the acetylene and

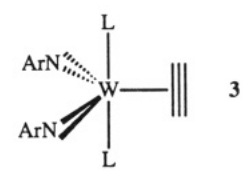

ethylene ligands are equivalent in each complex on the NMR time scale down to −80 °C, and the two phosphine ligands are equivalent. All data are consistent with their being approximate trigonal bipyramids that contain axial phosphine ligands and equatorial imido ligands. The N–W–N angle is likely to be ~150°, as it is in $Os(NAr)_2(PMe_2Ph)I_2$.[17] (See also Discussion later.) NMR data

(4) Jolly, M.; Mitchell, J. P.; Gibson, V. C. *J. Chem. Soc., Dalton Trans.* **1992**, 1329.
(5) Siemeling, U.; Gibson, V. C. *J. Organomet. Chem.* **1992**, *426*, C25.
(6) Dyer, P. W.; Gibson, V. C.; Howard, J. A. K.; Whittle, B.; Wilson, C. *J. Chem. Soc., Chem. Commun.* **1992**, 1666.
(7) Cockcroft, J. K.; Gibson, V. C.; Howard, J. A. K.; Poole, A. D.; Siemeling, U.; Wilson, C. *J. Chem. Soc., Chem. Commun.* **1992**, 1668.
(8) Poole, A. D.; Gibson, V. C.; Clegg, W. *J. Chem. Soc., Chem. Commun.* **1992**, 237.
(9) Glueck, D. S.; Green, J. C.; Michelman, R. I.; Wright, I. N. *Organometallics* **1992**, *11*, 4221.
(10) Schrock, R. R.; Murdzek, J. S.; Bazan, G. C.; Robbins, J.; DiMare, M.; O'Regan, M. *J. Am. Chem. Soc.* **1990**, *112*, 3875.
(11) Fox, H. H.; Yap, K. B.; Robbins, J.; Cai, S.; Schrock, R. R. *Inorg. Chem.* **1992**, *31*, 2287.
(12) Schrock, R. R.; DePue, R. T.; Feldman, J.; Yap, K. B.; Yang, D. C.; Davis, W. M.; Park, L. Y.; DiMare, M.; Schofield, M.; Anhaus, J.; Walborsky, E.; Evitt, E.; Krüger, C.; Betz, P. *Organometallics* **1990**, *9*, 2262.
(13) Williams, D. S.; Schrock, R. R. *Organometallics* **1993**, *12*, 1148.
(14) Toreki, R.; Vaughan, G. A.; Schrock, R. R.; Davis, W. M. *J. Am. Chem. Soc.* **1993**, *115*, 127.
(15) Horton, A. D.; Schrock, R. R. *Polyhedron* **1988**, *7*, 1841.
(16) Kool, L. B.; Rausch, M. D.; Alt, H. G.; Herberhold, M.; Thewalt, U.; Wolf, B. *Angew. Chem., Int. Ed. Engl.* **1985**, *24*, 394.
(17) Schofield, M. H.; Kee, T. P.; Anhaus, J. T.; Schrock, R. R.; Johnson, K. H.; Davis, W. M. *Inorg. Chem.* **1991**, *30*, 3595.

alone cannot distinguish whether acetylene and ethylene lie in the WN_2 plane or are oriented perpendicular to it; however, the molecular structure of $Mo(NAr)_2(PMe_3)_2(\eta^2\text{-}C_2H_4)$[18] reveals that the ethylene ligand is oriented perpendicular to the trigonal plane in an approximate trigonal bipyramid. Therefore we propose that the same is true in the case of **2** and **3**. (See drawing of **3**.) In related rhenium bis(pyridine) complexes (see later) the imido rings do not "rotate" rapidly on the NMR time scale about the C_{ipso}–N bond. The apparent rapid rotation of aryl rings in **3** might be ascribed to reversible formation of $W(NAr)_2(\eta^2\text{-}C_2H_4)L$ via loss of L from **3**, a type of species in which the aryl rings rotate readily on the NMR time scale (see **4** below).

$W(NAr)_2(PMe_2Ph)_2$ reacts with (trimethylsilyl)acetylene to form $W(NAr)_2(PMe_2Ph)(\eta^2\text{-}HC{\equiv}CSiMe_3)$ (**4**) (eq 2). NMR data suggest a rigid pseudotetrahedral geometry

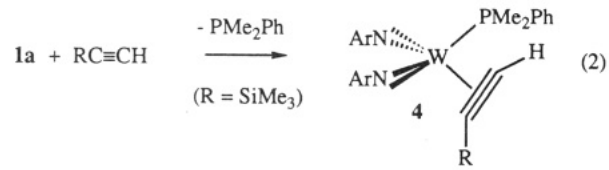

(2)

in which the carbon atoms of the alkyne ligand, tungsten, and the phosphorus atom all lie in a plane that bisects the N—W—N angle, a structure that would be analogous to that observed for $Mo(N\text{-}t\text{-}Bu)_2(CH_2{=}CHMe)(PMe_3)$.[6] The alkyne does not rotate about the metal–ligand(centroid) axis readily on the NMR time scale, and no coupling between the phosphine ligand and the alkyne carbon atoms is observed in the ^{13}C NMR spectrum. We speculate that the substituent in **4** is located in the "outside" or distal position, as shown in eq 2. The downfield resonances of the acetylenic protons (10.91 ppm), the downfield resonances of the coordinated carbon atoms (174 ppm), and the low value for ν_{CC} (1591 cm^{-1}) are all consistent with a strongly bound "dianion-like" alkyne.[19] We presume that a five-coordinate species analogous to **3** is untenable for steric reasons when R ≠ H.

Reactions between **1a** and olefins larger than ethylene also result in loss of phosphine and formation of η^2-olefin complexes. For example, addition of norbornene to **1a** gives $W(NAr)_2(PMe_2Ph)(\eta^2\text{-norbornene})$ (**5**). NMR data again suggest a pseudotetrahedral geometry in which the olefin does not rotate about the metal–olefin(centroid) axis and in which the two imido ligands are inequivalent. We propose that the phosphorus and two olefin carbon atoms lie in the plane that bisects the N–W–N angle.

Reactions between **1a** and aldehydes or ketones yield complexes that contain η^2-aldehyde or ketone ligands. For example $W(NAr)_2(PMe_2Ph)_2$ reacts within 1–2 min with acetone, propionaldehyde, or cyclopentanone to give orange-yellow $W(NAr)_2(PMe_2Ph)(\eta^2\text{-}OCMe_2)$ (**6a**), $W(NAr)_2(PMe_2Ph)(\eta^2\text{-}OCHEt)$ (**6b**) (eq 3), or $W(NAr)_2(PMe_2Ph)(\eta^2\text{-cyclopentanone})$ (**6c**). All NMR data are consistent with structures analogous to that shown in eq 3. Consequently, the two imido ligands are equivalent on the NMR time scale at 25 °C in **6a** and **6c**, while in **6b** they are inequivalent. Two isomers are observed for **6b**; in each isomer the two imido ligands are inequivalent and the methylene protons in propionaldehyde are diastereotopic. We propose that the isomers are those in which the oxygen is bound in the PCO plane either in the endo position, as shown in eq 3, or in the exo position.

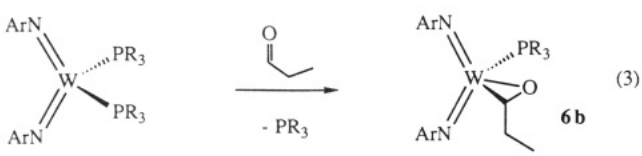

(3)

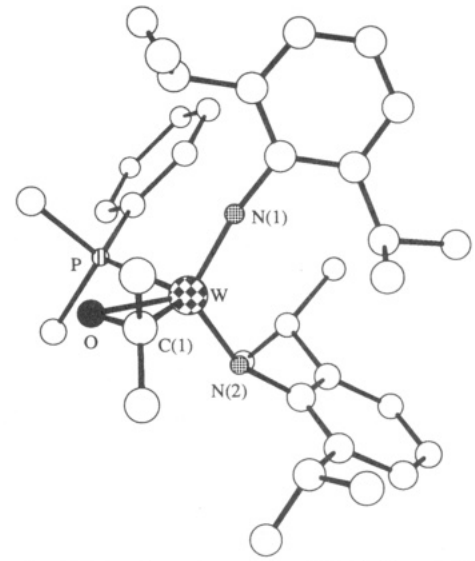

Figure 2. Molecular structure of $W(NAr)_2(PMePh)(\eta^2\text{-}OCMe_2)$ (**6a**).

Table II. Selected Bond Distances (Å) and Angles (deg) in $W(NAr)_2(PMe_2Ph)(\eta^2\text{-}OCMe_2)$ (6a)

	Distances		
W–N(1)	1.785(6)	W–P(1)	2.509(2)
W–N(2)	1.776(7)	W–O(1)	2.025(5)
W–C(1)	2.118(9)	O(1)–C(1)	1.39(1)
	Angles		
P(1)–W–O(1)	74.8(2)	N(1)–W–C(1)	108.8(3)
P(1)–W–N(1)	100.6(2)	N(2)–W–C(1)	110.8(3)
P(1)–W–N(2)	106.8(2)	W–O(1)–C(1)	74.1(4)
P(1)–W–C(1)	113.7(3)	W–N(1)–C(11)	168.8(6)
O(1)–W–N(1)	121.5(3)	W–N(2)–C(21)	155.8(5)
O(1)–W–N(2)	121.1(2)	W–C(1)–O(1)	66.8(4)
O(1)–W–C(1)	39.0(3)	W–C(1)–C(2)	118.2(7)
N(1)–W–N(2)	116.0(3)	W–C(1)–C(3)	121.2(6)

An X-ray study showed **6a** to have the proposed pseudotetrahedral structure in which W, P, O, and C all lie in the plane that bisects the N–W–N angle (mean deviation of 0.034 Å; Figure 2; Table II). One imido ligand is close to linear (W–N–C = 168.8 (6)°), while the other is more bent (155.8(5)°). Note that the imido groups' phenyl rings are oriented as they are in **1a**. The C–O distance of 1.39(1) Å suggests that **6a** is best described as an oxametallacyclopropane complex of W(VI). This description is consistent with the fact that no CO stretch could be observed in the IR spectrum above 1400 cm^{-1}. The η^2 bonding in **6a** is analogous to that found recently in other recently published η^2-bound ketone or aldehyde complexes.[20,21]

Synthesis of $Re(NAr)_2X$ Complexes. Reduction of $Re(NAr)_2Cl_3(py)$[15] (Ar = 2,6-C_6H_3-*i*-Pr_2) with 1 equiv of zinc or 2 equiv of sodium amalgam in the presence of excess pyridine in tetrahydrofuran yields brown, microcrystalline $Re(NAr)_2(py)_2Cl$ (**7**) in 80% yield. NMR spectra are

(18) Gibson, V. C. Personal communication.
(19) Templeton, J. L. *Adv. Organomet. Chem.* **1989**, *29*, 1.
(20) Bryan, J. C.; Mayer, J. M. *J. Am. Chem. Soc.* **1990**, *112*, 2298.
(21) Hill, J. E.; Fanwick, P. E.; Rothwell, I. P. *Organometallics* **1992**, *11*, 1771.

consistent with **7** being a trigonal bipyramid that contains axial pyridine ligands and imido aryl rings that lie in the equatorial plane. Presumably, the N—Re—N angle is large, as observed in $Os(NAr)_2(PMe_2Ph)I_2$ (N—Os—N = 151.2(3)°),[17] and free rotation of the aryl rings is restricted for steric reasons. Therefore the isopropyl groups that point toward the "inside" of the N=Re=N angle are not equivalent to the "outer" isopropyl groups on the NMR time scale in CD_2Cl_2 at 25 °C (see structure for **7** in eq 4),

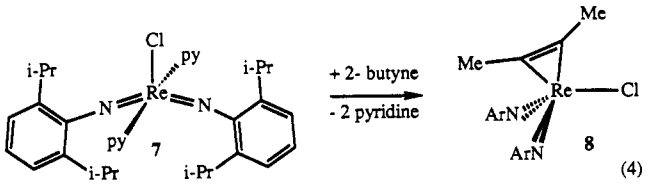

(4)

although in C_6D_6 at room temperature the appropriate resonances are simply broad. Coordinated pyridine does not exchange with free pyridine in **7** at a rate on the order of the NMR time scale up to 70 °C, but pyridine-d_5 exchanges readily with coordinated pyridine on the chemical time scale (15 min or less).

The addition of 2-butyne to **7** affords red $Re(NAr)_2(\eta^2\text{-}C_2Me_2)Cl$ (**8**). NMR spectra of **8** are consistent with a pseudotetrahedral geometry in which the ends of the coordinated alkyne ligand are inequivalent and the aryl rings rotate readily about the N–C_{ipso} bond (see below). This structure is analogous to that reported for compounds of the type $ReO_2(\eta^2\text{-}C_2R_2)R'$.[22] Olefins such as ethylene and norbornene do not displace the pyridine ligands in **7** readily, nor do ketones or aldehydes. The dineopentylacetylene analog of **8** has been reported elsewhere.[13]

One of the pyridine ligands in **7** is displaced readily by a phosphine to yield the emerald green compounds $Re(NAr)_2(L)(py)Cl$ (L = $PMePh_2$ (**9a**), PPh_3 (**9b**)). Excess phosphine does not displace the second pyridine ligand readily. Reduction of $Re(NAr)_2Cl_3(py)$ in the presence of $PMePh_2$ or PPh_3 also yields **9a** or **9b**. Compounds of type **9** appear to have structures analogous to that proposed for **7**; however, in **9a** and **9b** the ReN_2Cl plane is not a molecular plane of symmetry, as it is in **7**. Resonances for the isopropyl methyl groups are broad in C_6D_6 at 25 °C, suggesting that "rotation" of the aryl rings in **9** again is faster on the NMR time scale than it is in **7**, but slower than it is in **2** or **3**. The chloride ligand in compounds of type **9** can be removed with thallium tetrafluoroborate in THF in the presence of $PMePh_2$ to afford $[Re(NAr)_2(PMePh_2)_2][BF_4]$ (**10**). **10** is only slightly soluble in benzene or toluene but is freely soluble in THF. NMR data are consistent with a pseudotetrahedral core geometry.

Reduction of **7** with 2 equiv of sodium amalgam in THF in the presence of $PMePh_2$ in THF affords low yields of $Re(NAr)_2(PMePh_2)_2H$ (**11**), which can be isolated as midnight blue crystals. It is an analog of the known hydride complex $Re(NAr)_2(PMe_2Ph)_2H$[13] and is proposed to arise via protonation of "$[Re(NAr)_2(PMe_2Ph)_2]^-$." In **11** the hydride resonance is found at −9.72 ppm in the proton NMR spectrum. $[Re(NAr)_2(PMe_2Ph)_2]^-$ would be an analog of the known d^4 compound $Os(NAr)_2(PMe_2Ph)_2$[17] and would be expected to be a powerful base, since $[Re(NAr)_3]^-$ is a powerful base[13] compared to relatively unreactive $Os(NAr)_3$.[17] We propose that **11** has a structure analogous to that of **7** (eq 4).

(22) Felixberger, J. K.; Kuchler, J. G.; Herdtweck, E.; Paciello, R. A.; Herrmann, W. A. *Angew. Chem., Int. Ed. Engl.* **1988**, *27*, 946.

Rhenium(V) bis (imido) neopentyl derivatives are also prepared readily. Reduction of $Re(NAr)_2(CH_2\text{-}t\text{-}Bu)Cl_2$ by sodium amalgam or zinc in the presence of pyridine in THF yields green $Re(NAr)_2(CH_2\text{-}t\text{-}Bu)(py)_2$ (**12**). It is also possible to prepare **12** by treating **7** with dineopentylzinc. The imido resonances for **12** are sharp, in contrast to broad imido resonances observed for **7**, but the symmetry is similar, i.e., one in which the pyridine nitrogen atoms and neopentyl α carbon atoms lie in a plane that bisects the N=Re=N angle and the aryl rings of the imido ligands lie in the ReN_2 plane. Free pyridine does not exchange rapidly on the NMR time scale with coordinated pyridine in **12** at temperatures up to 70 °C, although added pyridine-d_5 exchanges in less than 10 min with coordinated pyridine at 25 °C. We speculate that pyridine exchanges on the chemical time scale via intermediate $Re(NAr)_2(CH_2\text{-}t\text{-}Bu)(py)$ that is formed by loss of pyridine from **12**; this exchange must be slow on the NMR time scale, as it is in **7**.

Compound **12** is much more reactive than **7**, perhaps in part because the bulk of the neopentyl group increases the lability of a pyridine ligand. 2-Butyne reacts rapidly with **12** to give $Re(NAr)_2(CH_2\text{-}t\text{-}Bu)(\eta^2\text{-}C_2Me_2)$ (**13a**), a species whose symmetry is similar to that of **8**, i.e., one in which the three carbon atoms bound to Re lie in a plane that bisects the N=Re=N angle. Analogous reactions between **7** and acetone, pivaldehyde, or norbornene give the dark yellow compounds $Re(NAr)_2(CH_2\text{-}t\text{-}Bu)(\eta^2\text{-}OCMe_2)$ (**13b**), $Re(NAr)_2(CH_2\text{-}t\text{-}Bu)(\eta^2\text{-}OCH\text{-}t\text{-}Bu)$ (**13c**), or $Re(NAr)_2(CH_2\text{-}t\text{-}Bu)(\eta^2\text{-norbornene})$ (**13d**), respectively, all of which appear to have structures analogous to **13a** and $W(NAr)_2(PMe_2Ph)(\eta^2\text{-}OCMe_2)$ (eq 5). No C—O

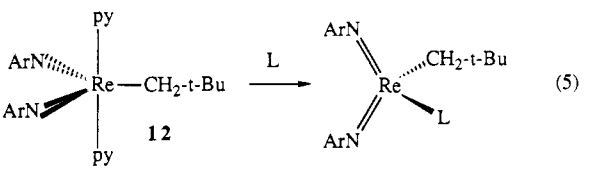

(5)

L = 2-butyne (**13a**), acetone (**13b**), pivaldehyde (**13c**), norbornene (**13d**), PMe_2Ph (**14**).

stretching frequency is observed for **13b** or **13c** above 1450 cm^{-1}. Compounds **13a–d** are all relatively stable in the absence of oxygen and moisture and may be stored indefinitely at −40 °C.

Reduction of $Re(NAr)_2(CH_2\text{-}t\text{-}Bu)Cl_2$ in the presence of PMe_2Ph gives $Re(NAr)_2(CH_2\text{-}t\text{-}Bu)(PMe_2Ph)$ (**14**) in 80% yield. Compound **14** may also be prepared by adding phosphine to **12** and removing the pyridine *in vacuo*. Free phosphine exchanges rapidly on the NMR time scale at 25 °C with coordinated phosphine in **14**, most likely via an associative mechanism to form intermediate $Re(NAr)_2(CH_2\text{-}t\text{-}Bu)(PMe_2Ph)_2$. Not surprisingly, therefore, **14** reacts readily with 2-butyne, norbornene, and propionaldehyde to afford **13a**, **13d**, and **13c**, respectively. However, in reactions between **14** and relatively small π-acceptor ligands such as ethylene, acetylene, and carbon monoxide, the phosphine ligand is retained in the coordination sphere of the product to give green $Re(NAr)_2(CH_2\text{-}t\text{-}Bu)(PMe_2Ph)(\eta^2\text{-}C_2H_4)$ (**15a**), red $Re(NAr)_2(CH_2\text{-}t\text{-}Bu)(PMe_2Ph)(\eta^2\text{-}C_2H_2)$ (**15b**), or blue-green $Re(NAr)_2(CH_2\text{-}t\text{-}Bu)(CO)(PMe_2Ph)$ (**15c**), respectively. Unfortunately, neither **15a** nor **15b** can be isolated. (Attempts to isolate **15a** by removing solvent in vacuo yielded only **14**; therefore **15a** could be observed only in the presence of ethylene.) NMR data for compounds **15** are consistent with structures analogous to that shown for **3** earlier. In each compound

Table III. Valence Molecular Orbitals of $W(NH)_2$[a]

level	energy, eV	occup[c]	charge distribution, %[b] W	N	H	W basis functions[d]
$6a_1$	−2.538	0	11	21	28	s(30) d_{x^2,y^2,z^2}(67) f(2)
$4b_1$	−2.972	0	22	23	30	d_{xz}(97) f(3)
$5a_1$	−3.059	0	45	8	1	s(8) p_z(4) d_{x^2,y^2,z^2}(88)
$2b_2$	−3.346	0	66	8	0	p_y(1) d_{yz}(98)
$4a_1$	−4.170	2	53	3	6	s(15) d_{x^2,y^2,z^2}(84)
$1b_2$	−7.619	2	16	62	1	p_y(12) d_{yz}(77) f(11)
$3b_1$	−7.628	2	12	66	3	p_x(22) d_{xz}(50) f(28)
$3a_1$	−8.148	2	22	56	2	s(5) p_z(9) d_{x^2,y^2,z^2}(83) f(3)
$1a_2$	−8.695	2	30	54	0	d_{xy}(97) f(3)
$2b_1$	−13.409	2	26	50	23	p_x(24) d_{xz}(70) f(6)
$2a_1$	−14.415	2	20	54	25	s(23) p_z(4) d_{x^2,y^2,z^2}(61) f(12)
$1b_1$	−20.698	2	22	71	7	p_x(43) d_{xz}(48) f(9)
$1a_1$	−22.350	2	30	66	3	s(28) p_z(8) d_{x^2,y^2,z^2}(45) f(18)

[a] Coordinate system is the same as in Figure 3. Levels above $4a_1$ are virtual (unoccupied) levels. [b] % of total charge density (not normalized) excluding inter-sphere and outer-sphere regions. [c] Occupancy in electrons. [d] Breakdown of spherical harmonics for tungsten basis functions.

there is a plane of symmetry that bisects the N=Re=N angle and the aryl rings rotate readily about the Re—N—C bond on the NMR time scale. It should be noted that the ethylene ligand in **15a** and the acetylene ligand in **15b** lie in the plane of symmetry; i.e., the ends of the ethylene ligand are inequivalent and the ends of the acetylene ligand are inequivalent; a proposed structure of **15b** is shown in eq 6.

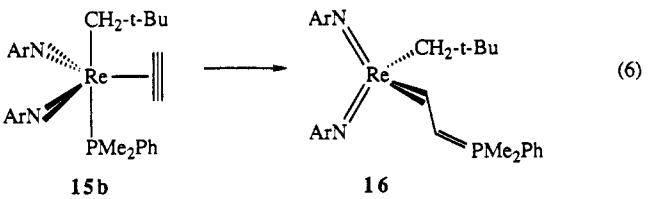

15b **16** (6)

Compound **15b** rearranges readily in solution to the "vinylalkylidene" complex $Re(NAr)_2(CH_2\text{-}t\text{-}Bu)(CHCHPMe_2Ph)$ (**16**; eq 6). The alkylidene H_α proton resonance in **16** is found at 12.14 ppm ($^3J_{H_aH_b}$ = 16.1 Hz and $^3J_{H_aP}$ = 29.8 Hz), the H_β resonance is found at 4.59 ppm ($^2J_{H_bP}$ = 36.2 Hz), and the C_α and C_β resonances are found at 222 ppm (J_{CH} = 130.2 Hz) and 72.7 ppm (J_{CH} = 167, $^1J_{PC}$ = 91 Hz), respectively. No $C_\alpha P$ coupling is observed. There is no plane of symmetry either relating the imido ligands or containing them, consistent with a pseudotetrahedral structure in which rotation about the Re=C bond is not fast (eq 6). These data are analogous to those obtained for other $Re(NAr)_2(CH\text{-}t\text{-}Bu)X$ (X = Cl, $CH_2\text{-}t\text{-}Bu$) complexes,[15] and with those for $ReO(CHCHPMe_3)(CH_2SiMe_3)_3$,[23] which was prepared in a reaction between $ReO(CH_2SiMe_3)_3(PMe_3)$ and acetylene.

Several other complexes in the $Re(NAr)_2X(L)$ (L = 2e donor) class have been reported elsewhere.[13] This list includes complexes of the type $Re(NAr)_2(NHAr)(L)$ (L = η^2-HC≡CH, η^2-MeC≡CMe, η^2-*t*-BuCHO, η^2-CH_2=CH_2, η^2-norbornene, PMe_3) and $Re(NAr)_2(\eta^2\text{-NpC}{\equiv}CNp)X$ (X = Me, CH_2-2,4,6-C_6H_2, H).

SCF-Xα-SW Analysis of $M(NH)_2(PH_3)_2$ (M = W, Re^+) Complexes. Table III lists the calculated ground-state two electron energies, occupation, charge distribution, and partial breakdown of the molecular orbitals for the 14-electron $W(NH)_2$ fragment in C_{2v} symmetry. The orientation and coordinate system for this model is shown in Figure 3. Wavefunction contour maps of the HOMO

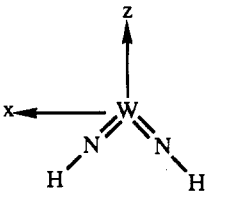

Figure 3. Orientation and coordinate system for the $W(NH)_2$ fragment in C_{2v} symmetry.

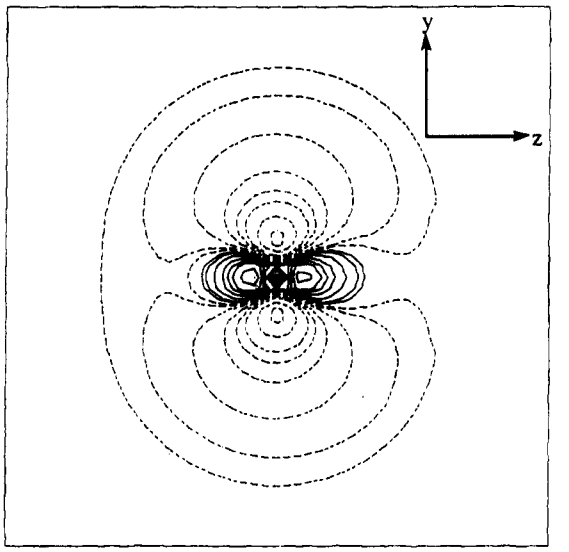

Figure 4. Wavefunction contour map of orbital $4a_1$ (HOMO) in the *yz* plane. Solid and dashed lines correspond to positive and negative signs for the wavefunction. Contours are drawn for charge densities ±0.4, ±0.2, ±0.15, ±0.1, ±0.075, ±0.5, ±0.025, ±0.01, ±0.005 $(e/bohr^2)^{1/2}$ (for all subsequent contour maps).

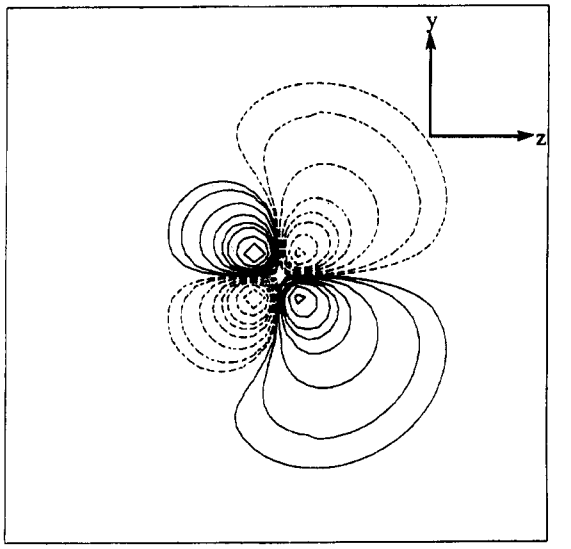

Figure 5. Wavefunction contour map of orbital $2b_2$ (LUMO) in the *yz* plane.

and the two lowest unoccupied MO's are shown in Figures 4–6. In the idealized structure all W–N–H angles are 180°, N–W–N = 120°, W–N = 1.78 Å (from the X-ray study of **1b**), and N–H = 1.36 Å.

The tungsten s, p_x, p_z, and d_{z^2} orbitals dominate the σ-interactions, mixing with the nitrogen σ orbitals to form the a_1 and the b_1 (σ) levels. The four orbitals which constitute W–N and N–H σ bonding transform as $2A_1 + 2B_1$. (A "pure" W–N σ molecular orbital is not separable from this set.) At higher energy are the π levels, with the out-of-plane $1a_2$ being the most stable. The HOMO ($4a_1$)

(23) Lappas, D.; Hoffman, D. M.; Folting, K.; Huffman, J. C. *Angew. Chem. Int., Ed. Engl.* **1988**, *27*, 587.

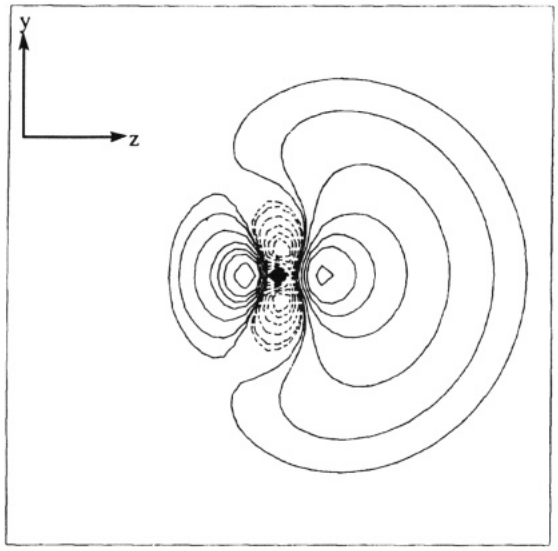

Figure 6. Wavefunction contour map of orbital $5a_1$ in the yz plane.

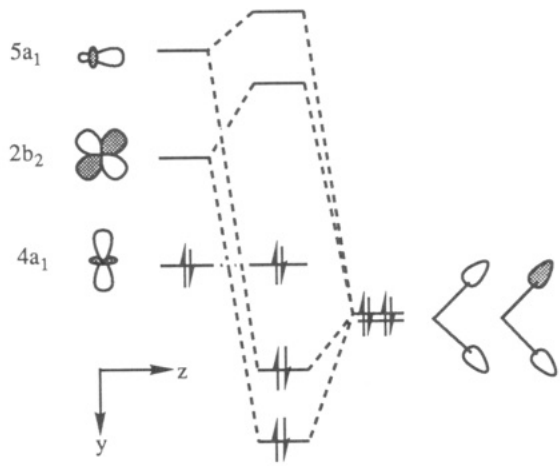

Figure 7. Interaction between frontier orbitals and ligand orbitals in $W(NH)_2L_2$.

consists largely of $d_{x^2-y^2}$ and d_{z^2} in a linear combination oriented along the y-axis. It is, in effect, a d_{y^2} orbital. The next two levels, $2b_2$ and $5a_1$, are separated by only ~0.3 eV. In a four-coordinate complex such as **1b** linear combinations of the phosphorus σ orbitals transform as $A_1 + B_2$. Interaction of the B_2 combination with the metal $2b_2$ is at a maximum when the P–W–P angle is 90°. The A_1 combination can interact with either the $4a_1$ or $5a_1$ metal orbital. Interaction with the $4a_1$ (which is at a maximum at 180°) is disfavored, as it results in the occupation of a high-lying σ^* orbital. Interaction with the $5a_1$ (which increases as the P–W–P angle decreases), on the other hand, is stabilizing. The small P–W–P angle observed in **1b** (95°) therefore is consistent with the HOMO being the $4a_1$ orbital and the σ bonds being formed using the $5a_1$ and $2b_2$ orbitals. An orbital interaction diagram summarizing these interactions is shown in Figure 7.

As depicted, the metal-centered HOMO is not expected to change on coordination of the phosphine ligands. A full SCF–Xα–SW calculation on $W(NH)_2(PH_3)_2$ (based on the structure of **1a**) revealed this to be the case. Table IV lists the calculated ground-state two electron energies, occupation, charge distribution, and partial breakdown of the molecular orbitals for $W(NH)_2(PH_3)_2$ in C_{2v}-symmetry. The orientation and coordinate system for this model is shown in Figure 8. A wavefunction contour map of the HOMO ($7a_1$) is shown in Figure 9. As shown in the table, the W–N–H σ and W–N π levels change only slightly. The gap between the highest W–N π orbital (b_2) and the HOMO ($4a_1$ in $W(NH)_2$ and $7a_1$ in $W(NH)_2(PH_3)_2$) drops slightly upon phosphine coordination. The orientation of the HOMO in $W(NH)_2(PH_3)_2$ (and $W(NH)_2$) ensures that unsaturated molecules will orient themselves in the yz plane for π back-bonding, as illustrated in the X-ray structure of **6a**.

A full SCF–Xα–SW calculation on hypothetical $[Re(NH)_2(PH_3)_2]^+$ was also performed using **1a** as a model.

Table IV. Valence Molecular Orbitals of $W(NH)_2(PH_3)_2$[a]

level	energy, eV	occup[c]	charge distribution, %[b] W	N	P	W basis functions[d]
$3a_2$	−1.418	0	43	20	7	d_{xy}(99) f(1)
$9a_1$	−1.534	0	8	6	4	s(2) d_{x^2,y^2,z^2}(92) f(7)
$5b_2$	−1.559	0	35	12	10	p_y(1) d_{yz}(98) f(1)
$8a_1$	−2.444	0	10	19	1	s(7) p_z(2) d_{x^2,y^2,z^2}(88) f(2)
$5b_1$	−2.727	0	19	22	3	d_{xz}(97) f(3)
$7a_1$	−3.686	2	49	3	9	s(1) p_z(2) d_{x^2,y^2,z^2}(97)
$4b_2$	−6.838	2	7	59	5	p_y(45) d_{yz}(38) f(17)
$4b_1$	−6.953	2	10	64	1	p_x(24) d_{xz}(52) f(25)
$6a_1$	−7.402	2	16	53	4	p_z(17) d_{x^2,y^2,z^2}(80) f(2)
$2a_2$	−8.018	2	27	52	1	d_{xy}(97) f(3)
$3b_2$	−8.542	2	24	3	53	p_y(5) d_{yz}(93) f(2)
$5a_1$	−9.022	2	18	3	52	s(41) p_z(6) d_{x^2,y^2,z^2}(51) f(2)
$2b_2$	−9.964	2	0	0	50	
$1a_2$	−10.093	2	1	0	50	
$3b_1$	−10.094	2	0	0	50	
$4a_1$	−10.209	2	1	0	50	
$2b_1$	−12.183	2	27	50	0	p_x(21) d_{xz}(74) f(5)
$3a_1$	−13.225	2	21	54	0	s(24) p_z(4) d_{x^2,y^2,z^2}(63) f(10)
$1b_2$	−18.274	2	0	0	61	
$2a_1$	−18.322	2	0	0	61	
$1b_1$	−19.503	2	17	74	0	p_x(43) d_{xz}(49) f(8)
$1a_1$	−20.897	2	24	71	0	s(30) p(8) d_{x^2,y^2,z^2}(46) f(16)

[a] Coordinate system is the same as in Figure 8. Levels above $7a_1$ are virtual (unoccupied) levels. [b] % of total charge density (not normalized) excluding inter-sphere and outer-sphere regions. [c] Occupancy in electrons. [d] Breakdown of spherical harmonics for tungsten basis functions.

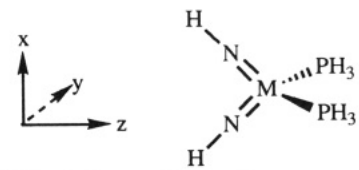

Figure 8. Orientation and coordinate system for model $M(NH)_2(PH_3)_2$ (M = W, Re^+) in C_{2v} symmetry.

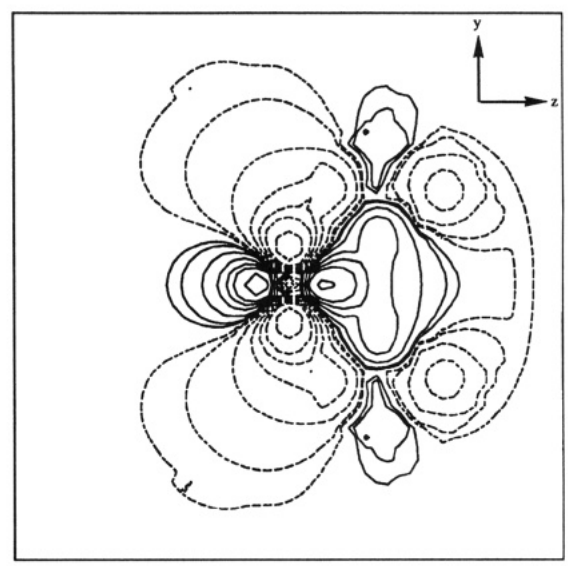

Figure 9. Wavefunction contour map of orbital $7a_1$ (HOMO) in the yz plane.

Table V. Valence Molecular Orbitals of $[Re(NH)_2(PH_3)_2]^{+a}$

level	energy, eV	occup[c]	charge distribution, %[b] Re	N	P	Re basis functions[d]
$5b_2$	−4.461	0	47	14	17	$p_y(1)\ d_{yz}(98)\ f(1)$
$8a_1$	−4.505	0	22	25	2	$s(1)\ d_{x^2,y^2,z^2}(98)\ f(1)$
$3a_2$	−4.786	0	48	32	3	$d_{xy}(99)\ f(1)$
$5b_1$	−5.277	0	27	21	2	$p_x(3)\ d_{xz}(96)\ f(2)$
$7a_1$	−6.727	2	54	7	7	$s(1)\ p_z(3)\ d_{x^2,y^2,z^2}(96)$
$4b_1$	−9.070	2	9	67	0	$p_x(27)\ d_{xz}(49)\ f(25)$
$4b_2$	−9.106	2	6	52	15	$p_y(70)\ d_{yz}(16)\ f(14)$
$6a_1$	−10.112	2	23	38	14	$s(3)\ p_z(14)\ d_{x^2,y^2,z^2}(83)$
$2a_2$	−10.646	2	35	45	3	$d_{xy}(98)\ f(2)$
$3b_2$	−11.034	2	37	9	38	$p_y(1)\ d_{yz}(97)\ f(1)$
$5a_1$	−11.277	2	26	10	39	$s(30)\ p_z(1)\ d_{x^2,y^2,z^2}(67)\ f(2)$
$2b_2$	−11.649	2	0	0	50	
$3b_1$	−11.726	2	0	0	51	
$1a_2$	−11.747	2	2	2	49	
$4a_1$	−11.894	2	2	1	51	
$2b_1$	−15.350	2	26	51	0	$p_x(15)\ d_{xz}(82)\ f(4)$
$3a_1$	−15.775	2	21	55	0	$s(24)\ p_z(4)\ d_{x^2,y^2,z^2}(61)\ f(10)$
$1b_2$	−20.081	2	0	0	61	
$2a_1$	−20.128	2	0	0	62	
$1b_1$	−22.617	2	21	73	0	$p_x(33)\ d_{xz}(60)\ f(6)$
$1a_1$	−23.560	2	25	71	0	$s(32)\ p(10)\ d_{x^2,y^2,z^2}(42)\ f(16)$

[a] Coordinate system is the same as in Figure 8. Levels above $7a_1$ are virtual (unoccupied) levels. [b] % of total charge density (not normalized) excluding inter-sphere and outer-sphere regions. [c] Occupancy in electrons. [d] Breakdown of spherical harmonics for rhenium basis functions.

Table V lists the calculated ground-state two electron energies, occupation, charge distribution, and partial breakdown of the molecular orbitals for $[Re(NH)_2(PH_3)_2]^+$ in C_{2v} symmetry. The results for $[Re(NH)_2(PH_3)_2]^+$ are similar to those obtained for $W(NH)_2(PH_3)_2$ with two noteworthy exceptions: First, the gap between the highest Re–N π orbital ($4b_2$) and the HOMO ($7a_1$) is smaller; the cationic nature of the complex would be expected to lower the energy of the metal orbitals relative to the nitrogen lone pairs, from which the π orbitals arise. Second, the distribution of π molecular orbitals ($6a_1$ and $2a_2$) is more heavily weighted toward the nitrogen atoms for the tungsten model than for rhenium, again suggesting that in the cationic complex, the π bond is not as polar because the d orbitals which are used to form the π bond are lower in energy than they are in the neutral tungsten complex.

The symmetry properties and relative energies of the frontier orbitals calculated for $W(NH)_2$ are analogous to those obtained for MCp_2 systems and therefore strongly support the proposed isolobal relationship between bent bis(imido) complexes[1,2,6,9] and bent metallocenes.[24-27] Furthermore, the trends in electron distribution for the frontier orbitals in $W(NH)_2$ match the trends in Cp_2M complexes.

In Figure 10 a Walsh diagram is shown for distortion of the $W(NH)_2$ fragment from a N–W–N angle of 120° to a N–W–N angle of 180°. (Relativistic effects are not included, so the energies shown in Figure 10 differ slightly from those listed in Table III.) Trans multiply-bonded ligands can participate in meaningful π bonding only through two d orbitals that are oriented along the ligand–M–ligand axis. Therefore as the N–M–N angle increases in $W(NH)_2$, the contribution of d character in two of the π bonds increases and, at the same time, the contribution of d character in the other two π bonds decreases. As shown, the four nondegenerate π levels ($1a_2$, $3a_1$, $1b_2$, and $3b_1$) evolve into two sets of doubly-degenerate π orbitals, one metal-based set and one ligand-based set. At the same time, the $5a_1$ and $2b_2$ orbitals yield a doubly-degenerate HOMO ($d_{y^2-z^2}$ and d_{yz} in this coordinate system).

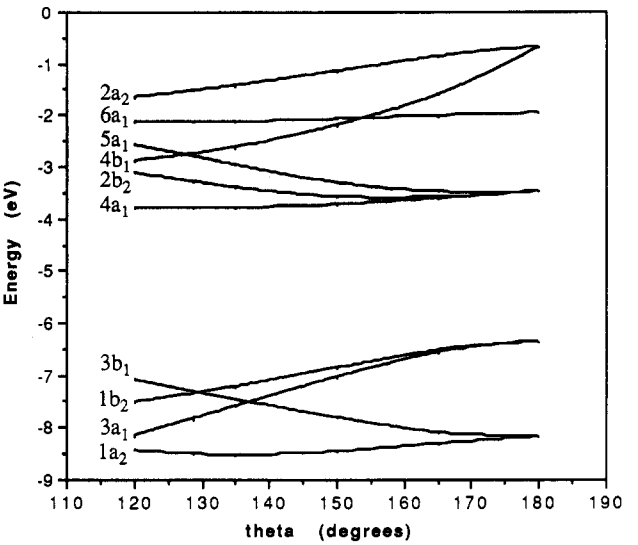

Figure 10. Walsh diagram for N–W–N angular distortion. (Relativistic effects not included.)

This correlation diagram is analogous to that calculated for bent or linear Cp_2M systems[26] and to that constructed for $Os(NAr)_2$ complexes[17] in order to rationalize the N–Os–N angle of ~150° in $Os(NAr)_2I_2(PMe_2Ph)$. In short, the N–M–N angle should increase from 120° in five-coordinate d^2 complexes in order to eliminate electron density in the π^* orbital, but if the angle increases to 180°, then only 16 electrons remain in metal-centered bonding orbitals; i.e., the metal is electron deficient. An N–M–N angle of ~150° is a compromise between the two undesirable extremes. The N–M–N angle in five-coordinate tungsten and rhenium bis(imido) complexes reported here is likely to be roughly the same as found in $Os(NAr)_2I_2(PMe_2Ph)$ for that reason. It is important to note that as the N–M–N angle increases, the b_2 (d_{yz}) orbital would be the only one available for back-bonding to an η^2 ligand in the trigonal (xz) plane in a five-coordinate bis(imido) complex in which the imido nitrogen atoms lie in the trigonal plane. In order for efficient back-bonding the η^2 ligand must be oriented perpendicular to the trigonal plane, as proposed in all bis(imido) species prepared here and as found in $Mo(NAr)_2(PMe_3)_2(\eta^2\text{-}C_2H_4)$.[18]

Discussion

The results presented here illustrate the isolobal analogy between 14 electron $W(NAr)_2$ and $M'Cp_2$ complexes where M′ is a group 4 metal. Each fragment has two frontier orbitals of a_1 symmetry and one of b_2 symmetry, and a HOMO of a_1 symmetry. For d^2 tungsten complexes of the type $W(NAr)_2$, the $M'Cp_2$ analogs would be d^2 MCp_2L_2 complexes (M = Ti, Zr, Hf). Such species are not as well-known as d^0 Cp_2MX_2 complexes, although they are becoming increasingly important components of group 4 metallocene chemistry.[16,28-32] When such species contain an η^2 ligand, it is generally proposed that the σ

(24) Petersen, J. L.; Lichtenberger, D. L.; Fenske, R. F.; Dahl, L. F. *J. Am. Chem. Soc.* **1975**, *97*, 6433.
(25) Brintzinger, H. H.; Lohr, L. L., Jr.; Tang Wong, K. L. *J. Am. Chem. Soc.* **1975**, *97*, 5146.
(26) Lauher, J. W.; Hoffmann, R. *J. Am. Chem. Soc.* **1976**, *98*, 1729.
(27) Albright, T. A.; Burdett, J. K.; Whangbo, M.-H. Orbital Interactions in Chemistry; Wiley & Sons: New York, 1985.
(28) Buchwald, S. L.; Kreutzer, K. A.; Fisher, R. A. *J. Am. Chem. Soc.* **1990**, *112*, 4600.
(29) Kreutzer, K. A.; Fisher, R. A.; Davis, W. M.; Spaltenstein, E.; Buchwald, S. L. *Organometallics* **1991**, *10*, 4031.
(30) Kool, L. B.; Rausch, M. D.; Alt, H. G.; Herberhold, M.; Honold, B.; Thewalt, U. *J. Organomet. Chem.* **1987**, *320*, 37.

bonding system involves the a_1 orbital that points along the z-axis and the b_2 orbital, leaving the a_1 orbital that points along the y-axis for π bonding to the η^2 ligand; therefore the η^2 ligand must lie in the xz plane (the plane that bisects the Cp–M–Cp angle). All evidence presented here suggests that the situation is similar in d^2 $M(NAr)_2$ complexes.

The conclusions drawn here for bis(imido) complexes also should hold for imido/alkylidyne and imido/cyclopentadienyl complexes. We mentioned in the Introduction several examples of the latter. Complexes of the type Re(C-*t*-Bu)(NAr)L_2(L = $PMePh_2$ or PMe_2Ph) have been prepared by reducing Re(C-*t*-Bu)(NAr)Cl_2L complexes with sodium amalgam in the presence of L,[33] so we might expect complexes of the type Re(C-*t*-Bu)(NAr)(η^2-ligand)L to be accessible. d^2 complexes having the W(η^5-C_5R_5)(C-*t*-Bu) core should be accessible via reduction of W(η^5-C_5R_5)(C-*t*-Bu)Cl_2 complexes.[34] In complexes that contain two different types of $2\pi,1\sigma$ ligands the $2\pi,1\sigma$ ligands are best treated as a unit rather than individually.

It is well-known that in d^2 complexes, such as $[ReO_2py_4]^+$, the oxo ligands are trans to one another, i.e., each oxo ligand behaves as a $1\pi,1\sigma$ ligand and the electron pair is in a d_{xy} orbital (if the z-axis is taken to be the O–M–O axis).[35] The scarcity of d^2 ME_2L_4 complexes in which E is an imido ligand might be attributed to the greater electron donating (π bonding) ability of imido ligands relative to oxo ligands as well as to steric congestion caused by the imido ligands' substituents.

The isolobal analogy[26,36] is, strictly speaking, a structural analogy. Therefore it will not predict to what extent *reactivity* pathways for bis(imido) compounds will resemble those for bis(cyclopentadienyl) compounds. One difference between $W(NAr)_2$ and $M'Cp_2$ complexes is that trigonal bipyramidal $W(NAr)_2L_2L'$ complexes can form readily. In such species a total of three metal–nitrogen π bonds, one filled d orbital, and five σ bonds are possible if a rehybridization takes place and the N–W–N angle increases to the point where the d_{yz} orbital is nonbonding, or is involved in back-bonding to an η^2 ligand. We can expect the N–W–N angle to be relatively large in such species in order to reduce the overall W–N bond order and minimize the destabilizing effect of that configuration. Ready attack on $W(NAr)_2L_2$ species by L', and the reverse, in theory could be an important part of a catalytic reaction, which in many cases involve interconversion of four- and five-coordinate species, i.e., a maximum electron count is more or less maintained at the metal during any four-coordinate/five-coordinate transformation (or vice versa). Another potentially important difference between $W(NAr)_2$ and $M'Cp_2$ complexes from a point of view of reactivity patterns is the likelihood that the imido ligand will less often be a "spectator" ligand[37] than the cyclopentadienyl ligand is commonly observed to be. In particular, the lone pair in an imido ligand is much more likely to be attacked by electrophiles.

Experimental Section

General Details. Standard experimental procedures can be found elsewhere.[13] All NMR chemical shifts are reported in ppm downfield from TMS (^1H, ^{13}C) or H_3PO_4 (^{31}P, $P(OMe)_3$ external reference, δ 141 ppm) in C_6D_6, unless stated otherwise (J values are in hertz). Infrared spectra were recorded as Nujol mulls between KBr plates. Microanalyses (C, H, N) were performed in our laboratory using a Perkin-Elmer PE2400 microanalyzer.

Preparation of Compounds. $W(NAr)_2(PMe_2Ph)_2$ (1a). $W(NAr)_2Cl_2$(dme) (3.50 g, 5.03 mmol) was dissolved in ether (60 mL), and dimethylphenylphosphine (1.39 g, 10.1 mmol) was added. This solution was chilled to −40 °C, and 0.5% Na/Hg (48.6 g, 10.57 mmol) was added. The mixture was shaken vigorously for 5 min and stirred overnight at room temperature. After ~16 h, the solution was decanted from the amalgam, filtered through Celite, and concentrated in vacuo. The resulting gel was extracted with toluene, and the extract was filtered through Celite and reduced to dryness in vacuo. The resulting residue was crystallized from pentane at −40 °C to give 1.97 g (48%) of dark purple product: ^1H NMR (toluene-d_8) δ 7.51 (br s, 4, PAr_o), 7.51–7.04 (overlapping multiplets, 12, $NAr_{m,p}$, $PAr_{m,p}$), 4.10 (sept, 4, C*H*Me_2), 1.65 (br s, 12, P*Me*$_2$Ph), 1.18 (d, 24, CH*Me*$_2$); ^{13}C NMR (toluene-d_8) δ 157.35 (NAr_i), 143.80 (PAr_i), 140.33, 137.40, 130.88, 129.31, 128.51, 122.38, 121.51 (NAr, $PAr_{o,m,p}$), 28.27 (*C*HMe$_2$), 25.02 (qd, J = 21, J = 125, P*Me*$_2$), 23.73 (CH*Me*$_2$); ^{31}P NMR (toluene-d_8) δ 17.30 (s, J_{PW} = 465). Anal. Calcd for $C_{40}H_{56}N_2P_2W$: C, 59.26; H, 6.96; N, 3.45. Found: C, 58.87; H, 7.17; N, 3.38.

$W(NAr)_2(PMePh_2)_2$ (1b). 1b was prepared in a manner analogous to that used to prepare 1a from $W(NAr)_2Cl_2$(dme) (0.500 g, 0.719 mmol), methyldiphenylphosphine (268 mL, 1.44 mmol), and 0.5% Na/Hg (6.9 g, 1.51 mmol); yield 302 mg (45%) of dark red crystals: ^1H NMR δ 7.51 (br t, 8, PAr_o), 7.17 (s, 6, $NAr_{m,p}$), 7.05–6.90 (overlapping t, 12, $PAr_{m,p}$), 4.12 (sept, 4, C*H*Me$_2$), 1.56 (virtual t, 6, P*Me*Ph$_2$), 1.13 (d, 24, CH*Me*$_2$). Anal. Calcd for $C_{50}H_{60}N_2P_2W$: C, 64.24; H, 6.47; N, 2.99. Found: C, 64.33; H, 6.41; N, 2.78.

$W(NAr)_2(PMe_2Ph)_2(\eta^2\text{-}C_2H_4)$ (2). $W(NAr)_2(PMe_2Ph)_2$ (180 mg, 222 μmol) was dissolved in ether (15 mL), and excess ethylene (10 mL gas) was added to the Schlenk flask under argon equipped with a rubber septum. The reaction was stirred for 10 min, during which time the dark red solution turned bright orange and the product began to precipitate. The solution was concentrated to approximately 4 mL in vacuo, and pentane was added to afford 145 mg (78% yield) of orange prisms: ^1H NMR δ 7.27 (m, 4, PAr_m), 7.11 (d, 4, NAr_m), 6.95 (m, 8, NAr_p, $PAr_{o,p}$), 3.67 (sept, 4, C*H*Me$_2$), 1.91 (s, C_2H_4), 1.33 (d, 12, $^3J_{PH}$ = 4.3, P*Me*$_2$Ph), 1.16 (d, 24, CH*Me*$_2$); ^{13}C NMR δ 140.55 (NAr_o), 131.0 (d, PAr), 129.21 (PAr), 128.61 (PAr), 122.74 (NAr_m), 121.90 (NAr_p), 31.2 (J_{CH} = 152, C_2H_4), 28.06 (*C*HMe$_2$), 23.83 (CH*Me*$_2$), 15.45 (d, $^1J_{PC}$ = 11, P*Me*$_2$Ph); ^{31}P NMR (toluene-d_8, −70 °C) δ −11.57 (J_{PW} = 232). Anal. Calcd for $C_{42}H_{60}N_2P_2W$: C, 60.14; H, 7.21; N, 3.34. Found: C, 60.31; H, 7.19; N, 3.01.

$W(NAr)_2(PMe_2Ph)_2(\eta^2\text{-}C_2H_2)$ (3). $W(NAr)_2(PMe_2Ph)_2$ (100 mg, 123 μmol) was dissolved in ether (8 mL), and excess acetylene (5 mL gas) was added to the vial equipped with a rubber septum. After 1 h the reaction was worked up as described fror 2; yield 74 mg (73%) of dark red prisms: ^1H NMR δ 10.24 (s, 2, H_2C_2), 7.48 (m, 4, PAr_m), 7.15 (d, 4, NAr_m), 7.0 (m, 8, NAr_p, $PAr_{o,p}$), 3.83 (sept, 4, C*H*Me$_2$), 1.30 (d, 12, $^3J_{PH}$ = 3, P*Me*$_2$Ph), 1.16 (d, 24, CH*Me*$_2$); ^{13}C NMR δ 156.31 (J_{CH} = 195, H_2C_2), 155.2 (NAr_i), 142 (NAr_o), 139.5 (PAr_i), 132.7 (PAr), 129.2 (PAr), 128.7 (PAr), 123.06 (NAr_p), 123.03 (NAr_m), 28.02 (*C*HMe$_2$), 23.59 (CH*Me*$_2$), 15.62 (P*Me*$_2$Ph). Anal. Calcd for $C_{42}H_{58}N_2P_2W$: C, 60.29; H, 6.99; N, 3.35. Found: C, 59.96; H, 7.04; N, 3.42.

(31) Buchwald, S. L.; Lum, R. T.; Dewan, J. C. *J. Am. Chem. Soc.* **1986**, *108*, 7441.
(32) Buchwald, S. L.; Watson, B. T.; Huffman, J. C. *J. Am. Chem. Soc.* **1987**, *109*, 2544.
(33) Williams, D. S. Ph.D. Thesis, Massachusetts Institute of Technology, 1993.
(34) Churchill, M. R.; Ziller, J. W.; McCullough, L. G.; Pedersen, S. F.; Schrock, R. R. *Organometallics* **1983**, *2*, 1046.
(35) Nugent, W. A.; Mayer, J. M. *Metal-Ligand Multiple Bonds*; Wiley: New York, 1988.
(36) Hoffmann, R. *Angew. Chem., Int. Ed. Engl.* **1982**, *21*, 711.
(37) Rappé, A. K.; Goddard, W. A. I. *J. Am. Chem. Soc.* **1982**, *104*, 3287.
(38) Siemeling, U.; Gibson, V. C. *J. Chem. Soc., Chem. Commun.* **1992**, 1670.

W(NAr)$_2$(PMe$_2$Ph)(η^2-Me$_3$SiC≡CH) (4). W(NAr)$_2$(PMe$_2$Ph)$_2$ (200 mg, 247 μmol) was dissolved in ether (8 mL), and (trimethylsilyl)acetylene (38.4 μL, 271 μmol) was added to the stirred solution. After 1 h the mixture was concentrated in vacuo and the resulting oil was recrystallized from pentane to afford 140 mg (74%) of orange prisms: ^{1}H NMR δ 10.91 (d, 1, J = 12.9, HC_2TMS), 7.46 (m, 2, PAr$_m$), 7.13 (m, 4, NAr$_m$), 7.01 (m, 2, NAr$_p$), 6.88 (m, 3, PAr$_{o,p}$), 3.83 (sept, 4, CHMe$_2$), 1.54 (d, 6, $^3J_{PH}$ = 9.5, PMe_2Ph), 1.14 (d, 12, CHMe_2), 1.13 (d, 12, CHMe'_2), 0.49 (s, 9, SiMe_3); ^{13}C NMR δ 174.20 (HCCTMS), 173.94 (HCCTMS), 154.70 (NAr$_i$), 142.02 (NAr$_o$), 132.03 (PAr$_o$), 130.78 (PAr$_p$), 128.95 (PAr$_m$), 123.08 (NAr$_p$), 122.34 (NAr$_m$), 27.72 (CHMe$_2$), 23.85 (CHMe_2), 23.70 (CHMe'_2), 17.28 (d, J = 37, PMe_2Ph), 1.01 (SiMe_3); ^{31}P NMR δ 15.22 (J_{PW} = 388); IR cm^{-1} 1591, 1586 (C≡C). Anal. Calcd for $C_{37}H_{55}N_2PSiW$: C, 57.66; H, 7.19; N, 3.64. Found: C, 58.02; H, 7.06; N, 3.64.

W(NAr)$_2$(PMe$_2$Ph)(η^2-norbornene) (5). W(NAr)$_2$(PMe$_2$Ph)$_2$ (200 mg, 247 μmol) was dissolved in ether (8 mL), and a solution of norbornene (26 mg, 271 μmol) in ether (1 mL) was added. The resulting red-yellow solution was stirred for 5 min and concentrated in vacuo to dryness. The resulting oil was recrystallized from pentane to afford 109 mg (48%) of orange prisms: ^{1}H NMR δ 7.42 (m, 2, PAr$_o$), 7.11 (m, 4, NAr$_m$), 7.04 (m, 2, NAr$_p$), 6.93 (m, 3, PAr$_{m,p}$), 4.02 (sept, 2, CHMe$_2$), 3.70 (sept, 2, CH'Me$_2$), 3.39 (dd, 1, J = 8.73, 3.2, HC_α), 3.28 (br s, 1, HC_β), 2.49 (br s, 1, $HC_{\beta'}$), 2.13 (dd, 1, J = 9.0, 9.0, $HC_{\alpha'}$), 1.98 (m, 2), 1.62 (dd, 6, J = 9.6, 2.7, PMe_2Ph), 1.60 (br m, 2), 1.18 (d, 6, CHMe_2), 1.17 (d, 6, CHMe'_2), 1.13 (d, 6, CHMe''_2), 1.11 (d, 6, CHMe'''_2), 0.705 (dt, 1) (other NBE proton not located); ^{13}C NMR δ 155.45 (NAr$_i$), 154.34, (NAr$_i$), 143.67 (NAr$_o$), 140.17 (NAr$_i$), 134.98 (d, J = 46.5, PAr$_i$), 131.16 (d, J = 11.5, PAr$_o$), 130.40 (PAr$_p$), 128.91 (d, J = 8.6, PAr$_m$), 124.13 (NAr$_p$), 122.53 (NAr$_m$), 122.47 (NAr$_m$), 121.91 (NAr$_p$), 89.1 (Cα), 89.0 (Cα'), 61.20, 61.07, 52.77, 45.48, 42.94, 37.37, 33.90, 22.65, 14.21 (NBE carbons), 28.19 (CHMe$_2$), 27.70 (C$'$HMe$_2$), 24.38 (CHMe_2), 23.96 (CHMe'_2), 23.90 (CHMe''_2), 23.34 (CHMe'''_2), 17.91 (d, J = 36.5, PMe_2Ph), 16.20 (d, J = 32, PMe'_2Ph); ^{31}P NMR δ 13.53 (J_{PW} = 362). Anal. Calcd for $C_{39}H_{55}N_2PW$: C, 61.10; H, 7.23; N, 3.66. Found: C, 61.38; H, 7.38; N, 3.31.

W(NAr)$_2$(PMe$_2$Ph)(η^2-Me$_2$CO) (6a). W(NAr)$_2$(PMe$_2$Ph)$_2$ (259 mg, 319 μmol) was dissolved in pentane (10 mL), and acetone (23 mg, 380 μmol) was added. Within 2 min, the solution had turned from dark red to yellow-orange. The solution was concentrated to ~5 mL in vacuo and cooled to −40 °C to give 150 mg (65%) of yellow crystals: ^{1}H NMR δ 7.42 (m, 2, PAr$_o$), 7.11 (m, 4, NAr$_m$), 7.0 (m, 2, NAr$_p$), 6.88 (m, 3, PAr$_{m,p}$), 3.91 (sept, 4, CHMe$_2$), 2.62 (d, 6, J = 1, OCMe_2), 1.61 (d, 6, J = 10.3, PMe_2Ph), 1.09 (d, 12, CHMe_2), 1.08 (d, 12, CHMe'_2); ^{13}C NMR δ 153.91 (NAr$_i$), 142.29 (NAr$_o$), 131.78 (d, J = 10.9, PAr$_o$), 131.18 (PAr$_p$), 129.20 (d, J = 8.9, PAr$_m$), 123.77 (NAr$_p$), 122.59 (NAr$_m$), 82.16 (OCMe$_2$), 32.90 (OCMe_2), 27.70 (CHMe$_2$), 24.16 (CHMe_2), 24.06 (CHMe'_2), 12.62 (d, J = 29, PMe_2Ph); ^{31}P NMR δ 12.16 (J_{PW} = 337). Anal. Calcd for $C_{35}H_{51}ON_2PW$: C, 57.54; H, 7.04; N, 3.84. Found: C, 57.92; H, 7.10; N, 3.72.

W(NAr)$_2$(PMe$_2$Ph)(η^2-EtCHO) (6b). W(NAr)$_2$(PMe$_2$Ph)$_2$ (200 mg, 247 μmol) was dissolved in ether (10 mL), and propionaldehyde (26.7 μL, 371 μmol) was added. After 10 min the reaction mixture was concentrated to ~1 mL, 2 mL of pentane was added, and 76 mg (42%) of dark yellow crystals were filtered off: ^{1}H NMR δ 7.44 (m, 2, PAr$_o$), 7.12 (m, 4, NAr$_m$), 7.03 (m, 2, NAr$_p$), 6.87 (m, 3, PAr$_{m,p}$), 4.65 (m, 1, HCO), 4.05 (sept, 2, CHMe$_2$), 3.77 (sept, 2, CH'Me$_2$), 3.36 (m, 1, HCHMe), 2.25 (m, 1, HCHMe), 1.57 (dd, 6, J = 10.2, 5.9, PMe_2Ph), 1.33 (t, 3, MeCH$_2$), 1.16 (d, 6, CHMe_2), 1.11 (d, 12, CHMe'_2, CHMe''_2), 1.07 (d, 6, CHMe'''_2); ^{13}C NMR δ 154.78 (NAr$_i$), 153.80, (NAr$_i$), 144.38 (NAr$_o$), 140.47 (NAr$_i$), 131.98 (d, J = 11.9, PAr$_o$), 131.32 (PAr$_p$), 129.20 (d, J = 10.3, PAr$_m$), 124.96 (NAr$_p$), 122.68 (NAr$_p$), 122.60 (NAr$_m$), 122.20 (NAr$_m$), 80.65 (OCHEt), 33.05 (OCCH$_2$Me), 27.96 (CHMe$_2$), 27.36 (C$'$HMe$_2$), 23.60 (CHMe_2, CHMe'_2), 23.49 (CHMe''_2), 22.95 (CHMe'''_2), 14.05 (MeCH$_2$), 13.61 (d, J = 32, PMe_2Ph), 11.03 (d, J = 31); ^{31}P NMR δ 13.01 (J_{PW} = 343). Anal. Calcd for $C_{35}H_{51}ON_2PW$: C, 57.54; H, 7.04; N, 3.84. Found: C, 57.72; H, 7.18; N, 3.51.

W(NAr)$_2$(Me$_2$PhP)[η^2-O=C(CH$_2$)$_4$] (6c). W(NAr)$_2$(PMe$_2$Ph)$_2$ (100 mg, 123 μmol) was dissolved in ether (7 mL), and cyclopentanone (10.9 mL, 123 μmol) was added. This was allowed to stir overnight. The resulting dark yellow-brown solution was filtered through Celite, washed with ether, and concentrated in vacuo. The yellow solid obtained was extracted in pentane, the solution was filtered and allowed to crystallize at −40 °C to yield 40 mg (43%) of yellow crystals: ^{1}H NMR δ 7.41 (m, 2, PAr$_m$), 7.11 (m, 4, NAr$_m$), 7.04 (m, 2, NAr$_p$), 6.85 (m, 3, PAr$_{o,p}$), 3.91 (sept, 4, CHMe$_2$), 3.13, 2.37, 2.15–1.93 (each m, total 8, OC(CH_2)$_4$), 1.58 (d, 6, J = 10.2, PMe_2Ph), 1.10 (dd, 24, CHMe_2).

Re(NAr)$_2$(py)$_2$Cl (7). Re(NAr)$_2$Cl$_3$(py) (6.126 g, 8.825 mmol) was dissolved in THF (30 mL) and added to a solution of pyridine (2.855 mL, 35.3 mmol) in THF (10 mL) over freshly prepared sodium amalgam (408 mg, 17.7 mmol of Na, 82 g of Hg). The mixture was shaken vigorously for 5 min and allowed to stir overnight. The brown solution was decanted from the amalgam, filtered through Celite, and concentrated in vacuo. The resulting brown oil was extracted with toluene, and the extract was filtered through Celite and concentrated in vacuo. The residue was extracted with ether (30 mL), and the extract was filtered through Celite and concentrated in vacuo to afford 4.23 g (68%) of a brown powder which is essentially pure by NMR: ^{1}H NMR δ 8.50 (d, 4, ortho), 7.28 (d, 4, meta), 6.98 (t, 2, para), 6.20 (t, 4, meta), 6.02 (t, 2, para), 3.85 (br s, 4, CHMe$_2$), 1.26 (br d, 24, CHMe_2). In CD_2Cl_2 the imido ligands show inequivalencies characteristic of slow rotation about the N–C bonds. Anal. Calcd for $ReC_{34}H_{44}N_4Cl$: C, 55.91; H, 6.07; N, 7.67. Found: C, 55.86; H, 6.06; N, 7.61.

Re(NAr)$_2$(η^2-C$_2$Me$_2$)Cl (8). 2-Butyne (214 μL, 2.74 mmol) was added to a red-brown solution of 1 (200 mg, 274 μmol) in benzene. The solution gradually lightened in color, giving a clear red-orange solution. The solution was stirred for 1 h, after which the solvent was removed slowly in vacuo to give red crystals of 8 (125 mg, 73%): ^{1}H NMR δ 7.00 (s, 6, aryl), 3.68 (sept, 4, CHMe$_2$), 2.92 (s, 3, MeCCMe), 2.53 (s, 3, MeCCMe), 1.13 (CHMe_2); ^{13}C NMR (CD_2Cl_2) δ 156.2 (MeCCMe), 152.7 (ipso), 143.8 (ortho), 141.9 (MeCCMe), 127.9 (para), 123.0 (meta), 28.7 (CHMe$_2$), 23.5 (12, CHMe_AMe$_B$), 23.2 (12, CHMe$_A$$Me_B$), 18.8 and 12.7 ($Me$CCMe and MeCC$Me$). Anal. Calcd for $ReC_{28}H_{40}N_2Cl$: C, 53.70; H, 6.44; N, 4.47. Found: C, 53.82; H, 6.40; N, 4.80.

Re(NAr)$_2$(py)(PMePh$_2$)Cl (9a). Re(NAr)$_2$Cl$_3$(py) (0.500 g, 0.720 mmol) was dissolved in THF (10 mL) and added to a solution of methyldiphenylphosphine (134 μL, 0.720 mmol) in THF (2 mL) over freshly prepared sodium amalgam (33 mg, 1.5 mmol of Na, 6.6 g of Hg). The mixture was shaken vigorously for 5 min and allowed to stir for 4 h. The green solution was decanted from the amalgam and filtered through Celite, and the extract was concentrated in vacuo. The residue was extracted with ether and the extract was filtered through Celite and concentrated to yield 0.417 g (68 %) of a green powder: ^{1}H NMR δ 8.56 (d, 2, ortho), 7.51 (dd, 4, ortho), 7.15 (d, 4, meta), 6.95 (m, 8, meta and para), 6.40 (t, 1, para), 6.24 (dd, 2, meta), 3.47 (br s, 4, CHMe$_2$), 2.02 (d, 3, PMe), 1.12 (br s, 24, CHMe_2); ^{31}P NMR δ −17.0 (s). Anal. Calcd for $C_{42}H_{52}N_2PClRe$: C, 59.24; H, 6.16; N, 4.94. Found: C, 59.39; H, 6.23; N, 4.93.

Re(NAr)$_2$(py)(PPh$_3$)Cl (9b). Re(NAr)$_2$Cl$_3$py (0.500 g, 0.720 mmol) was dissolved in THF (15 mL) with triphenylphosphine (0.189 g, 0.720 mmol), NEt$_4$Cl (0.119 g, 0.720 mmol), and Zn dust (47 mg, 0.720 mmol). The mixture was stirred vigorously overnight. The green solution was filtered through Celite, and the filtrate was concentrated in vacuo. The residue was extracted with toluene and the extract was filtered and concentrated in vacuo to afford 526 mg (80%) of a green powder: ^{1}H NMR δ 8.56 (d, 2, ortho), 7.66 (dd, 4, ortho), 7.16–6.90 (m, 12, various arom), 6.48 (t, 1, para), 6.27 (dd, 2, meta), 3.47 (sept 4, CHMe$_2$), 1.04 (br s, 24, CHMe_2); ^{31}P NMR δ 9.0 (br). Anal. Calcd for $C_{47}H_{54}N_3PClRe$: C, 61.79; H, 5.96; N, 4.60. Found: C, 61.75; H, 6.09; N, 4.66.

[Re(NAr)$_2$(PMePh$_2$)$_2$]BF$_4$ (10). TlBF$_4$ (34 mg, 120 μmol) was added to a solution of Re(NAr)$_2$(py)(PMePh$_2$)Cl (100 mg, 117 μmol) and dimethylphenylphosphine (21.9 μL, 117 μmol) in THF (5 mL). The solution was stirred overnight, during which

time it turned dark red and a white precipitate formed. The mixture was chilled to −40 °C and filtered through cold Celite. The filtrate was reduced to dryness to yield 116 mg (98%) of a maroon solid which was >95% pure by NMR: ^{1}H NMR δ 7.44 (dd, 8, ortho), 7.16 (t, 2, para), 7.1–7.0 (m, 12, arom), 6.94 (d, 4, meta), 3.32 (sept, 4, C*H*Me$_2$), 2.29 (d, 6, P*Me*), 0.84 (d, 24, CH*Me*$_2$); ^{1}H NMR (CD_2Cl_2) δ 7.59 (m, 4, arom), 7.51 (m, 8, arom), 7.34 (t, 2, para), 7.17 (d, 4, meta), 3.23 (sept, 4, C*H*Me$_2$), 1.82 (d, 6, P*Me*), 0.91 (d, 24, CH*Me*$_2$). Anal. Calcd for $C_{50}H_{60}N_2P_2BF_4Re$: C, 58.65; H, 5.91; N, 2.74. Found: C, 58.46; H, 5.95; N, 2.47.

Re(NAr)$_2$(PMePh$_2$)$_2$H (11). 7 (500 mg, 690 μmol) was added to a stirred THF (10 mL) solution of diphenylmethylphosphine (260 μL, 1400 μmol) over freshly prepared sodium amalgam (35 mg of Na, 1500 μmol, 4 g of Hg). The solution was shaken vigorously for 5 min and then stirred overnight. The mixture was taken to dryness in vacuo, and the residue was extracted with toluene. The extract was filtered through Celite, and the solvent was removed in vacuo. The residue was extracted with ether and the extract was concentrated to afford 100 mg (15%) of blue crystals: ^{1}H NMR δ 7.67 (m, 8, ortho), 7.05–6.85 (br m, 18, arom), 3.58 (br sept, 4, C*H*Me$_2$), 1.71 (br s, 6, P*Me*), 1.01 (d, 24, CH*Me*$_2$), −9.72 (br s, 1, Re*H*); ^{31}P NMR δ −7.97 (br s). Anal. Calcd for $C_{50}H_{61}N_2P_2Re$: C, 63.87; H, 6.54; N, 2.98. Found: C, 63.58; H, 6.58; N, 2.92.

Re(NAr)$_2$(CH$_2$-*t*-Bu)(py)$_2$ (12). A solution of Re(NAr)$_2$(CH$_2$-*t*-Bu)Cl$_2$ (2.500 g, 3.68 mmol) and NEt$_4$Cl (610 mg, 3.68 mmol) in THF (25 mL) was added to a slurry of Zn dust (325 mesh, 0.29 g, 4.5 mmol) in THF (2 mL). The emerald green solution was stirred overnight and filtered. The solvent was removed from the filtrate in vacuo and the residue was recrystallized from ether by adding pentane to give 1.65 g (49%) of dark green microcrystals: ^{1}H NMR δ 8.62 (d, 4, ortho), 7.34 and 7.23 (d, 2 each, meta), 7.06 (t, 2, para), 6.16 (t, 2, para), 6.06 (t, 4, meta), 4.45 and 3.84 (sept, 2 each, C*H*Me$_2$), 3.38 (s, 2, C*H*$_2$-*t*-Bu), 1.47 (d, 12, CH*Me*$_A$Me$_B$), 1.16 (d, 12, CHMe$_A$*Me*$_B$), 1.25 (s, 9, t-Bu); ^{13}C NMR (CD_2Cl_2) δ 156.2 (ipso), 153.6 (ortho), 139.9 (ortho), 136.9 (para), 124.1 (meta), 123.6 (para), 120.2 (meta), 66.2 (*C*H$_2$CMe$_3$), 39.4 (CH$_2$*C*Me$_3$), 33.7 (CH$_2$C*Me*$_3$), 28.6 and 27.1 (*C*HMe$_2$), 25.0 and 24.0 (CH*Me*$_2$). Anal. Calcd for $C_{39}H_{55}N_4Re$: C, 61.15; H, 7.24; N, 7.31. Found: C, 61.29; H, 7.35; N, 7.34.

Re(NAr)$_2$(CH$_2$-*t*-Bu)(η^2-MeC≡CMe) (13a). 2-Butyne (214 μL, 2.74 mmol) was added to an emerald green benzene solution of 7 (2.74 μmol) at room temperature. The solution turned brown and then lightened to red. After 1 h, the solvent was removed in vacuo and the residue was recrystallized from pentane at −40 °C to give red crystals (125 mg, 73%): ^{1}H NMR (CD_2Cl_2) δ 7.10 (s, 6, arom), 3.64 (s, 2, C*H*$_2$-*t*-Bu), 3.57 (sept, 4, C*H*Me$_2$), 2.88 (s, 3, *Me*CCMe), 2.67 (s, 3, MeCC*Me*), 1.24 (d, 12, CH*Me*$_A$Me$_B$), 1.13 (d, 12, CHMe$_A$*Me*$_B$), 1.08 (s, 9, *t*-Bu); ^{13}C NMR (CD_2Cl_2) δ 153.5 (ipso), 145.6 (MeCCMe), 145.4 (ortho), 140.3 (MeCCMe), 126.5 (para), 123.0 (meta), 43.6 (*C*H$_2$-*t*-Bu), 36.8 (CH$_2$*C*Me$_3$), 33.5, 28.2, 23.8, 23.5 (CH$_2$C*Me*$_3$, *C*HMe$_2$, CH*Me*$_A$Me$_B$, CHMe$_A$*Me*$_B$), 18.5 and 9.8 (*Me*CCMe and MeCC*Me*). Anal. Calcd for $C_{33}H_{51}N_2Re$: C, 59.88; H, 7.77; N, 4.23. Found: C, 59.63; H, 7.80; N, 4.29.

Re(NAr)$_2$(CH$_2$-*t*-Bu)(η^2-norbornene) (13b). Re(NAr)$_2$(CH$_2$-*t*-Bu)(py)$_2$ (100 mg, 127 μmol) was dissolved in ether (8 mL), and a solution of norbornene (12 mg, 127 μmol) in ether (1 mL) was added to the stirred solution. After 14 h the solution was filtered and taken to dryness in vacuo. The residue was recrystallized from pentane to afford 45 mg (50%) of yellow crystals: ^{1}H NMR δ 7.04 (m, 4, meta), 6.96 (d, 2H, para), 4.19 (d, 1, J = 7.7, H_α), 3.96 (sept, 2, J = 6.9, C*H*Me$_2$), 3.82 (s, 2, C*H*$_2$-*t*-Bu), 3.64 (sept, 2, J = 6.9, C*H*′Me$_2$), 3.12 (d, 1, J = 7.7, H_α′), 2.77 (br s, 1, H_β), 2.74 (br s, 1, H_β), 1.91 (ddd, 1), 1.61 (ddd, 1), 1.53 (ddd, 1), 1.37 (d, 6, J = 6.8, CH*Me*$_2$), 1.28 (s, 9, CH$_2$C*Me*$_3$), 1.26 (d, 6, J = 6.9, CH*Me*′$_2$), 1.21 (d, 6, J = 6.8, CH*Me*″$_2$), 1.13 (d, 6, J = 6.9, CH*Me*‴$_2$), 0.89 (br d, 1), 0.40 (d, 1), (other NBE proton was not located); ^{13}C NMR δ 186.1 (ipso), 145.31 (ortho), 143.89 (ipso), 126.67 (para), 125.69 (para), 123.32 (meta), 123.17 (meta), 68.80 (*C*H$_2$-*t*-Bu), 52.58 (NBE), 44.70 (NBE), 41.52 (NBE), 39.94 (*C*Me$_3$), 36.32 (NBE), 35.92 (NBE), 33.57 (C*Me*$_3$), 31.44 (NBE), 31.02 (NBE), 28.06 (*C*HMe$_2$), 27.88 (*C*′HMe$_2$), 24.33 (CH*Me*$_2$), 24.18 (CH*Me*′$_2$), 23.59 (CH*Me*″$_2$), 22.97 (CH*Me*‴$_2$). Anal. Calcd for $C_{36}H_{55}N_2Re$: C, 61.59; H, 7.90; N, 3.99. Found: C, 61.50; H, 7.73; N, 3.65.

Re(NAr)$_2$(CH$_2$-*t*-Bu)(η^2-OCH-*t*-Bu) (13c). Re(NAr)$_2$(CH$_2$-*t*-Bu)(py)$_2$ (120 mg, 152 μmol) was dissolved in ether (10 mL), and pivaldehyde (16.5 μL, 152 μmol) was added. The solution was allowed to stir for ~10 h, filtered, and concentrated in vacuo. The resulting brown oil was crystallized from pentane to yield 64 mg (59%) of yellow crystals: ^{1}H NMR δ 6.98 (d, 6, arom), 4.91 (s, 1, *H*CO), 3.88 (d, 1, J = 11.5, *H*CH-*t*-Bu), 3.74 (sept, 2, J = 6.8, C*H*Me$_2$), 3.73 (sept, 2, J = 6.8, C*H*′Me$_2$), 3.49 (d, 1, J = 11.5, *H*CH-*t*-Bu), 1.43 (s, 9, OCH-*t*-Bu), 1.25 (d, 6, J = 6.8, CH*Me*$_2$), 1.20 (d, 6, J = 6.8, CH*Me*′$_2$), 1.18 (s, 9, CH$_2$-*t*-Bu), 1.12 (d, 6, J = 6.8, CH*Me*″$_2$), 1.05 (d, 6, J = 6.8, CH*Me*‴$_2$); ^{13}C NMR δ 152.75 (ipso), 152.00 (ipso), 144.56 (ortho), 142.85 (ortho), 127.61 (para) 126.69 (para), 123.28 (meta), 123.07 (meta), 90.25 (J = 167, O*C*H-*t*-Bu), 50.57 (*C*H$_2$-*t*-Bu), 36.47, 36.16 (CH$_2$*C*Me$_3$, OCH*C*Me$_3$), 34.58 (CH$_2$C*Me*$_3$), 29.06 (OCHC*Me*$_3$), 28.65 (*C*HMe$_2$), 28.28 (*C*′HMe$_2$), 25.06 (CH*Me*$_2$), 24.10 (CH*Me*′$_2$), 23.15 (CH*Me*″$_2$), 23.10 (CH*Me*‴$_2$). Anal. Calcd for $C_{34}H_{55}N_2ORe$: C, 58.84; H, 7.99; N, 4.04. Found: C, 58.68; H, 8.01; N, 4.28.

Re(NAr)$_2$(CH$_2$-*t*-Bu)(η^2-OCMe$_2$) (13d). Re(NAr)$_2$(CH$_2$-*t*-Bu)(py)$_2$ (50 mg, 127 μmol) was dissolved in toluene (10 mL) and acetone (9.3 μL, 127 μmol) was added. After 2 h the solvents were removed from the solution in vacuo to give a green oil: ^{1}H NMR δ 6.99 (m, 6, arom), 3.79 (sept, 4, J = 6.9, C*H*Me$_2$), 3.73 (s, 2, C*H*$_2$-*t*-Bu), 2.46 (s, 6, OC*Me*$_2$), 1.38 (s, 9, CH$_2$C*Me*$_3$), 1.16 (d, 12, J = 6.9, CH*Me*$_2$), 1.14 (d, 12, J = 6.9, CH*Me*′$_2$); ^{13}C NMR δ 152.37 (ipso), 144.30 (ortho), 127.11 (para), 123.25 (meta), 85.22 (O*C*Me$_2$), 53.36 (*C*H$_2$-*t*-Bu), 36.84 (CH$_2$*C*Me$_3$), 33.68 (CH$_2$C*Me*$_3$), 31.38 (OC*Me*$_2$), 28.82 (*C*HMe$_2$), 23.60 (CH*Me*$_2$), 23.41 (CH*Me*′$_2$).

Re(NAr)$_2$(CH$_2$-*t*-Bu)(PMe$_2$Ph) (14). A slurry of Zn dust (241 mg, 3.68 μmol) in THF (2 mL) was added a solution of Re(NAr)$_2$(CH$_2$-*t*-Bu)Cl$_2$ (2.500 g, 3.683 mmol) and NEt$_4$Cl (610 mg, 3.683 mmol) in THF (25 mL). PMe$_2$Ph (524 μL, 3.683 μmol) was added, and the mixture was stirred overnight. The dark green reaction mixture was taken to dryness in vacuo, and the residue was extracted with ether. The extract was filtered through Celite, and and the filtrate was taken to dryness in vacuo. The dark residue was extracted with pentane, and the extract was filtered through Celite. The solution was cooled to −40 °C to give 1.96 g (71%) of dark green obsidian-like crystals: ^{1}H NMR δ 7.45 (m, 2, ortho), 7.20 (t, 2, para), 7.06 (d, 4, meta), 4.14 (s, 2, C*H*$_2$-*t*-Bu), 3.93 (sept, 4, C*H*Me$_2$), 1.57 (d, 6, J = 10.5, P*Me*$_2$Ph), 1.40 (s, 9, CH$_2$C*Me*$_3$), 1.23 (d, 12, CH*Me*$_2$), 1.19 (d, 12, CH*Me*′$_2$); ^{13}C NMR δ 156.53 (ipso), 142.58 (ortho), 140.1 (d, ipso), 131.90 (d, ortho), 130.34 (para), 128.40 (d, meta), 124.11 (para) 123.25 (meta), 37.71 (*C*H$_2$-*t*-Bu), 34.24 (CH$_2$C*Me*$_3$), 28.49 (*C*HMe$_2$), 23.95 (CH*Me*$_2$), 21.29 (CH$_2$C*Me*$_3$), 20.17 (d, P*Me*$_2$Ph); ^{31}P NMR (C_6D_6) δ 2.95 (s). Anal. Calcd for $C_{37}H_{56}N_2PRe$: C, 59.57; H, 7.57; N, 3.76. Found: C, 59.82; H, 7.68; N, 3.50.

Re(NAr)$_2$(CH$_2$-*t*-Bu)(PMe$_2$Ph)(η^2-C$_2$H$_4$) (15a). This compound can be observed by NMR upon adding excess ethylene (3 mL) to an NMR tube contaning Re(NAr)$_2$(CH$_2$-*t*-Bu)(PMe$_2$Ph) (50 mg, 67 μmol) in C_6D_6. It is stable only in the presence of excess ethylene. ^{1}H NMR δ 7.36 (m, 1, para), 7.14–6.97 (complex, 15, arom), 3.75 (s, 2, C*H*$_2$CMe$_3$), 3.75 (sept, 4, C*H*Me$_2$), 2.94 (t, 2, J = 12.4, ReC*H*$_2$CH′$_2$), 2.37 (t, 2, J = 12.4, ReCH$_2$C*H*′$_2$), 1.27 (d, 12, CH*Me*$_2$), 1.21 (s, 9, CH$_2$C*Me*$_3$), 1.15 (d, 12, CH*Me*′$_2$); ^{13}C NMR δ 153.3 (ipso), 145.3 (ortho), 131.0 (d, ortho), 130.9 (para), 128.4 (d, meta), 126.7 (para), 123.0 (meta), 44.47 (*C*H$_2$C′H$_2$), 35.9 (*C*H$_2$-*t*-Bu), 33.7 (CH$_2$C*Me*$_3$), 28.5 (*C*HMe$_2$), 27.4 (CH$_2$*C*Me$_3$), 24.2 (CH*Me*$_2$), 15.6 (P*Me*$_2$Ph); ^{31}P NMR δ −38 (br).

Re(NAr)$_2$(CH$_2$-*t*-Bu)(PMe$_2$Ph)(η^2-C$_2$H$_2$) (15b). This compound was observed by NMR in C_6D_6 upon adding acetylene (approximately 3 mL, 140 μmol) via syringe to an NMR tube containing Re(NAr)$_2$(CH$_2$-*t*-Bu)(PMe$_2$Ph) (100 mg, 134 μmol) in C_6D_6. It begins to decompose to 11 within 10 min at 25 °C: ^{1}H NMR δ 9.71 (t, 1, J_{PH} = 1.5, ReC*H*CH′), 9.35 (s, 1, ReCHC*H*), 7.36 (m, 2, ortho), 7.10 (m, 3, meta, para), 7.02 (s, 6, meta, para),

4.02 (d, 2, J_{PH} = 1.4, CH_2CMe_3), 3.65 (sept, 4, $CHMe_2$), 1.19 (d, 12, $CHMe_2$), 1.17 (2, 12, $CHMe_2'$), 1.16 (s, 9, CH_2CMe_3).

Re(NAr)$_2$(CH$_2$-*t*-Bu)(CO)(PMe$_2$Ph) (15c). Re(NAr)$_2$(CH$_2$-*t*-Bu)(PMe$_2$Ph) (200 mg, 268 μmol) was dissolved in ether in a high vacuum tube, and the solution was taken through three freeze–pump–thaw cycles. The tube was then pressurized to a pressure of 40 mmHg at 77 K (321 μmol of CO). The vessel was then sealed and warmed to room temperature. An intense blue color was observed as the solution melted. After 4 h the solvents were removed invacuo and the residue was extracted with ether. The extract was cooled to −40 °C to afford 108 mg (52%) of dark blue-green microcrystals: ^{1}H NMR δ 7.43 (m, 2, ortho) 7.19 (t, 2, para), 7.05 (d, 4, meta), 6.91 (m, 3, meta, para), 4.16 (s, 2, CH_2CMe_3), 3.91 (sept, 4, $CHMe_2$), 1.57 (d, 6, PMe_2), 1.39 (s, 9, CMe_3), 1.20 (br d, 24, $CHMe_2$); IR 1978 cm^{-1} (ν_{CO}). Anal. Calcd for $C_{38}H_{56}N_2OPRe$: C, 58.97; H, 7.29; N, 3.62. Found: C, 59.07; H, 7.77; N, 3.10.

Re(NAr)$_2$(CH$_2$-*t*-Bu)(CHCHPMe$_2$Ph) (16). Re(NAr)$_2$(CH$_2$-*t*-Bu)(PMe$_2$Ph) (300 mg, 402 μmol) was dissolved in ether (10 mL) in a vial and equipped with a septum cap. Acetylene (12 μL, 400 μmol) was introduced via syringe and the solution was stirred. After 5 min the solution had turned yellow, and after 1 h it had turned red. Solvents were removed in vacuo, and the resulting residue was extracted into pentane. The extract was filtered through Celite and cooled to −40 °C to give 164 mg (55%) of red chunky crystals: ^{1}H NMR δ 12.14 (dd, 1, J_{HH} = 16.1, J_{PH} = 29.8, ReCHCHPMe$_2$Ph), 7.25–7.10 (m, 8, arom), 6.95 (m, 2, ortho), 4.59 (dd, 1, J_{HH} = 16.1, J_{PH} = 36.2, ReCHCHPMe$_2$Ph), 4.18 (sept, 2, $CHMe_2$), 4.07 (sept, 2, $CH'Me_2$), 3.78 (d, 1, J = 13, ReCHH'CMe$_3$), 3.59 (d, 1, J = 13, ReCHH'CMe$_3$), 1.42 (s, 9, CH_2CMe_3), 1.4–1.25 (4 overlapping doublets, 24, $CHMe_2$), 0.86 (d, 3, J_{PH} = 12.7, PMeMe′), 0.82 (d, 3, J_{PH} = 12.7, PMeMe'); ^{13}C NMR δ 222.2 (J_{CH} = 130.2, ReCH), 150.1 (ipso), 145.6, 141.6, 132.1, 130.9 (d), 129.2, and 122.7 (all aromatic), 72.7 (d, J_{PC} = 91, J_{CH} = 167), 34.2 (CMe_3), 32.6 (ReCH_2CMe_3), 28.9 and 28.8 ($CHMe_2$), 23.7 ($CHMe_2$); ^{31}P NMR δ 11.7; IR 1583 cm^{-1} (ν_{CC}). Anal. Calcd for $C_{39}H_{58}N_2PRe$: C, 60.67; H, 7.57; N, 3.63. Found: C, 60.28; H, 7.46; N, 3.35.

SCF-Xα-SW Calculations. All calculations were carried out on either a Silicon Graphics or VAX workstation using a program based on the original Xα–SW code of K. H. Johnson and F. C. Smith, Jr.[39,40] A set of atomic coordinates (1 bohr = 0.529 177 Å) was first generated for each model in idealized geometry (C_{2v} for $W(NH)_2$, $W(NH)_2(PH_3)_2$, and $Re(NH)_2(PH_3)_2^+$). Sets of atomic sphere radii were calculated according to the Norman criterion[41] and were uniformly scaled until a satisfactory viral ratio ($-2T/V$ = 1.000 00) was obtained in the final calculation. Exchange correlation parameters (α values) were taken directly (for α_N, α_P) or interpolated (for α_W and α_{Re}) from Schwarz,[42,43] except for α_H where the value suggested by Slater[44] was used. The α values for the outer-sphere and interatomic regions were calculated as the weighted average of the α values for the constituent atoms, based on the number of valence electrons for each atom. The wavefunctions were expanded from partial waves (atomic angular momenta) on each atomic center where the l_{max} for each center was as follows: outer sphere and interatomic region, 5; tungsten and rhenium, 3; nitrogen and phosphorus, 2; hydrogen, 1. A molecular potential was generated by the superposition of atomic potentials, and this potential was used for the spin-restricted calculation of an initial set of wavefunctions. The levels were populated according to Fermi statistics, and a new molecular potential was generated. A fraction of the new potential was mixed in with the old potential, and the resulting potential was used as the starting point for the next calculation. This eliminated dramatic fluctuations in the molecular potential as the model reached self-consistency. The relativistic correction of Wood and Boring[45] was applied.

Calculations on the model $W(NH)_2(PH_3)_2$ in C_{2v} employed the following internal coordinates: W–N–H = 180°, N–W–N = 128.8°, W–N = 1.78 Å, W–P = 2.40 Å, P–W–P = 94° (from the X-ray study of **1b**), N–H = 1.07 Å, H–P–H = 93.3°, P–H = 1.42 Å. The sphere radii were optimized as above ($-2T/V$ = 1.000 005), and the results were corrected for relativistic effects. For the Walsh diagram depicted in Figure 10, full SCF–Xα–SW calculations (as described above) were conducted by employing the same sphere radii and interatomic distances used for $W(NH)_2$, varying the N–W–N angle from 120 to 180° in 15-deg increments. In the region that closely matches the model derived from **1b** (N–W–N = 128.8°) there were only minor differences in relative energies of the orbitals with and without a relativistic correction. For this reason, the results of the calculations were not corrected for relativistic effects.

Tables containing atomic coordinates, α values, and atomic sphere radii for the models $W(NH)_2$ and $W(NH)_2(PH_3)_2$ with N–W–N = 128.8° (from the X-ray structure of **1b**) are included in the supplemental material (Tables S1 and S2).

The calculations on the model $[Re(NH)_2(PH_3)_2]^+$ in C_{2v} were carried out as follows: Coordinates were selected on the basis of known rhenium bis(imido) complexes and the structure of the neutral tungsten analog (**1b**). Internal coordinates are Re–N = 1.71 Å, Re–P = 2.40 Å, N–H = 1.07 Å, P–H = 1.38 Å, N–Re–N = 128.8°, P–Re–P = 94°. After the sphere radii were optimized (as described above, $-2T/V$ = 1.000 001), the complex was enclosed within a negatively charged "Watson" sphere of radius 10.0 au, to simulate the counterion in a lattice environment. The calculation was converged to self-consistency and corrected for relativistic effects. A table (Table S3) containing atomic coordinates, α values, and atomic sphere radii for this model is included in the supplemental material.

Crystal Structure of W(NAr)$_2$(PMePh$_2$)$_2$ (1b). A dark red triclinic crystal of dimensions 0.10 × 0.20 × 0.20 mm was mounted on a glass fiber under a stream of cold nitrogen gas evaporated from a liquid nitrogen bath, and the data were collected at −72 °C by Dr. W. M. Davis on a Rigaku AFC6R diffractometer with graphite-monochromated Mo Kα radiation (λ = 0.710 69 Å). Of the 8228 reflections that were collected, 7819 were unique, and equivalent reflections were merged. The intensities of three representative reflections measured after every 150 reflections remained constant throughout data collection (no decay correction was applied). Cell constants and an orientation matrix for data collection, obtained from a least-squares refinement using the setting angles of 25 carefully centered reflections, corresponded to a triclinic cell with dimensions a = 12.417(4) Å, b = 18.406(4) Å, c = 11.087(4) Å, and α = 102.01(3)°, β = 112.06(2)°, and γ = 83.18(2)° for Z = 2 and fw = 934.84 ($WC_{50}H_{60}N_2P_2$); the calculated density is 1.353 g/cm^3. An empirical absorption correction, using the program DIFABS, was applied, resulting in relative transmission factors ranging from 0.86 to 1.18.

The structure was solved by the Patterson method. The final cycle of full-matrix least-squares refinement was based on 4898 observed reflections ($I > 3.00\sigma(I)$) and 496 variable parameters and converged (largest parameter shift was 0.00 times its esd) with unweighted and weighted agreement factors of R = 0.032 and R_w = 0.040. The maximum and minimum peaks on the final difference Fourier correspond to +0.79 and −1.20 e/Å^3, respectively.

Crystal Structure of W(NAr)$_2$(PMe$_2$Ph)(η^2-OCMe$_2$) (6a). The yellow prismatic crystals were stable in air for approximately 36 h. They were mounted on glass fibers under ambient conditions and coated with epoxy. The intensities of three representative reflections were measured after every 60 min of X-ray exposure time. The crystal was unstable in the beam and decayed in an accelerating fashion. Hence, the first crystal (dimensions 0.25 × 0.25 × 0.25 mm) failed to survive (>40% decay) first shell data collection. A second crystal (same dimensions) was used to complete the shell. The entire data set was processed in parts and corrected for decay (40% crystal no. 1, 25% crystal no. 2) and then appended. This treatment precluded the correction for absorption.

(39) Johnson, K. H. *Adv. Quantum Chem.* **1973**, *7*, 143.
(40) Case, D. *Annu. Rev. Phys. Chem.* **1982**, *33*, 151.
(41) Norman, J. G. *Mol. Phys.* **1976**, *31*, 1191.
(42) Schwarz, K. *Phys. Rev. B: Solid State* **1972**, *5*, 2466.
(43) Schwarz, K. *Theor. Chim. Acta* **1974**, *34*, 225.
(44) Slater, J. C. *Int. J. Quantum Chem.* **1973**, *S7*, 533.
(45) Wood, J. H.; Boring, A. M. *Phys. Rev. B* **1978**, *18*, 2701.

All measurements were made on an Enraf-Nonius CAD-4 diffractometer with graphite-monochromated Mo Kα radiation (λ = 0.710 69 Å). All calculations were performed using the TEXSAN crystallographic software package of Molecular Structure Corp. Cell constants and an orientation matrix for data collection, obtained from a least-squares refinement using the setting angles of 25 carefully centered reflections in the range 12.00° <2θ < 18.00°, corresponded to a monoclinic cell with dimensions a = 16.714(1) Å, b = 12.343(1) Å, c = 16.966(1) Å, and β = 91.909(7)° for Z = 4 and fw = 730.62 ($WC_{35}H_{51}ON_2P$); the calculated density is 1.387 g/cm^3. On the basis of the systematic absences of $h01$, $h \neq 2n$, and $0k0$, $k \neq 2n$, the space group was determined to be $P2_1/a$. The data were collected at 24 ± 1 °C using the ω scan technique to a maximum 2θ value of 44.9°. ω scans of several intense reflections, made prior to data collection, had an average width at half-height of 0.28° with a takeoff angle of 2.8°. Scans of (0.80 + 0.35 tan θ)° were made at speeds ranging from 0.9 to 8.0°/min (in ω). Moving-crystal moving-counter background measurements were made by scanning an additional 25% above and below the scan range. The counter aperture consisted of a variable horizontal slit with a width ranging from 3.0 to 3.5 mm and a vertical slit set to 4.0 mm. The diameter of the incident beam collimator was 0.8 mm, and the crystal–detector distance was 17.3 cm. For intense reflections an attenuator (attenuation factor = 17.93) was automatically inserted in front of the detector.

Of the 5011 reflections which were collected, 4819 were unique (R_{int} = 0.035); equivalent reflections were merged. The data were corrected for Lorentz and polarization effects.

The structure was solved by a combination of the Patterson method and direct methods. The non-hydrogen atoms were refined anisotropically. The final cycle of full-matrix least-squares refinement was based on 3319 observed reflections ($I > 3.00\sigma(I)$) and 362 variable parameters and converged (largest parameter shift was 0.00 times its esd) with unweighted and weighted agreement factors of R = 0.037 and R_w = 0.037. The maximum and minimum peaks on the final difference Fourier correspond to +0.63 and −0.98 e/Å^3, respectively.

Acknowledgment. We thank the National Science Foundation (CHE 91 22827) for supporting this research, Dr. William Davis for collecting the data sets for **1b** and **6a**, and Dr. Ira Weinstock for the original synthesis of $Re(NAr)_2(py)_2Cl$.

Supplementary Material Available: Labeled ORTEP drawings and tables of final positional parameters, final thermal parameters, and Xα parameters and coordinates for models $W(NH)_2$ (S1), $W(NH)_2(PH_3)_2$ (S2), and $[Re(NH)_2(PH_3)_2]^+$ (S3) (16 pages). Ordering information is given on any current masthead page. (Supplementary material for **6a** has already been deposited.[1])

OM930367V